© 2021. Published by The Company of Biologists Ltd | Development (2021) 148, dev199224. doi:10.1242/dev.199224

RESEARCH ARTICLE

Piecemeal regulation of convergent neuronal lineages by bHLH transcription factors in *Caenorhabditis elegans*

Neda Masoudi[1], Eviatar Yemini[1], Ralf Schnabel[2] and Oliver Hobert[1,*]

ABSTRACT

Cells of the same type can be generated by distinct cellular lineages that originate in different parts of the developing embryo ('lineage convergence'). Several *Caenorhabditis elegans* neuron classes composed of left/right or radially symmetric class members display such lineage convergence. We show here that the *C. elegans* Atonal homolog *lin-32* is differentially expressed in neuronal lineages that give rise to left/right or radially symmetric class members. Loss of *lin-32* results in the selective loss of the expression of pan-neuronal markers and terminal selector-type transcription factors that confer neuron class-specific features. Another basic helix-loop-helix (bHLH) gene, the Achaete-Scute homolog *hlh-14*, is expressed in a mirror image pattern relative to *lin-32* and is required to induce neuronal identity and terminal selector expression on the contralateral side of the animal. These findings demonstrate that distinct lineage histories converge via different bHLH factors at the level of induction of terminal selector identity determinants, which thus serve as integrators of distinct lineage histories. We also describe neuron-to-neuron identity transformations in *lin-32* mutants, which we propose to also be the result of misregulation of terminal selector gene expression.

KEY WORDS: *C. elegans*, Lineage, Neuronal differentiation, Transcriptional control

INTRODUCTION

The complete lineage map of every individual cell in the nematode *Caenorhabditis elegans* provides an excellent opportunity to study how lineage affects cellular identity (Sulston and Horvitz, 1977; Sulston et al., 1983). One intriguing revelation of the lineage description is that phenotypically similar cells can have different lineage histories. This is particularly evident in the nervous system, composed of 302 neurons in the *C. elegans* hermaphrodite. Based on anatomy, function and molecular profiles, these 302 neurons can be grouped into 118 different classes, with members of each class being phenotypically similar and often completely indistinguishable by any known criterion (Hobert et al., 2016; Taylor et al., 2021; White et al., 1986). Members of individual neuron classes can have very similar lineage histories. For example, many ventral cord motor neuron classes are composed of members with similar lineage histories (Sulston et al., 1983). Many classes of bilaterally symmetric neuron pairs also comprise two members with similar developmental history (Sulston et al., 1983). However, members of the same neuron class can also have very distinct lineage histories. For example, the four bilaterally symmetric cephalic CEP sensory neurons, composed of a bilaterally symmetric ventral neuron pair (CEPV left and CEPV right) and a bilaterally symmetric dorsal neuron pair (CEPD left and CEPD right), share similar overall morphology, similar patterns of synaptic connectivity (White et al., 1986) and similar molecular composition (Taylor et al., 2021). However, the CEPD pair and CEPV pair derive from different neuroblast lineages (Sulston et al., 1983). Members of other radially symmetric neuron classes are also phenotypically indistinguishable, despite distinct lineage histories; for example, the IL1, IL2 and OLQ neuron classes are composed of ventral and dorsal pairs that each have distinct lineage histories (Sulston et al., 1983). Even neuron classes that are only composed of two bilaterally symmetric neurons can be derived from two lineally distinct neuroblasts. For example, the left and right ASE neurons derive from different embryonic blastomeres (ABa and ABp) (Sulston et al., 1983). Thus, distinct lineage histories can converge on similar neuronal identities. Similar lineage convergence phenomena have also recently been observed in vertebrates (Cao et al., 2019; Chan et al., 2019; McKenna et al., 2016; Wagner et al., 2018). For example, specific types of excitatory and inhibitory neurons of the mouse central nervous system (CNS) develop through multiple, convergent trajectories (Cao et al., 2019).

How is such convergence achieved? Based on studies of neuronal identity control, one point of convergence of distinct lineage histories are terminal selector transcription factors, which are post-mitotically expressed master regulators of neuron identity (Hobert, 2016). For example, the two lineally distinct ASE neurons both eventually turn on the terminal selector CHE-1, which instructs ASE neuron identity (Hobert, 2014). Similarly, all six members of the IL2 neuron class, despite their distinct lineage histories, co-express the terminal selectors *unc-86*, *sox-2* and *cfi-1*, which cooperate to control the expression of IL2 identity features (Shaham and Bargmann, 2002; Vidal et al., 2015; Zhang et al., 2014). Similarly, the left and right CAN neurons, which display nonsymmetric, distinct lineage histories, co-express the *ceh-10* homeobox gene, required to specify the identity of both these neurons (Forrester et al., 1998; Wenick and Hobert, 2004). These observations indicate that different lineage histories converge on the expression of similar terminal selectors and, therefore, that terminal selectors are integrators of distinct lineage histories. What then are the molecular factors that converge in a lineage-specific manner to drive individual terminal selectors in a neuron type-specific manner?

Recent single cell RNA (scRNA) analysis of developing embryos revealed molecular correlates to distinct lineage histories, such that the precursors of cells with similar terminal identities were shown to display distinct gene expression profiles, exactly as predicted by their distinct lineage histories (Packer et al., 2019; Sulston et al., 1983). In this paper, we show that the *C. elegans* Atonal homolog

[1]Department of Biological Sciences, Columbia University, Howard Hughes Medical Institute, New York, NY 10027, USA. [2]Institute of Genetics, Technische Universität Braunschweig, 38106 Braunschweig, Germany.

*Author for correspondence (or38@columbia.edu)

E.Y., 0000-0003-1977-0761; O.H., 0000-0002-7634-2854

Handling editor: Swathi Arur
Received 20 February 2021; Accepted 29 April 2021

Development (2021) 148, dev199224. doi:10.1242/dev.199224

lin-32 (Zhao and Emmons, 1995) is differentially expressed in distinct lineages of cells that phenotypically converge on the same neuronal cell classes and selectively affects the specification of only some class members. Moreover, we discovered that the Achaete-Scute homolog *hlh-14* (Frank et al., 2003) displays a mirror image expression pattern relative to *lin-32* and functions on the contralateral side of the animal.

Our analysis of basic helix-loop-helix (bHLH) transcription factors was originally motivated by our quest to understand how the expression of terminal selector transcription factors is controlled. Terminal selectors have emerged as key regulators of neuronal identity throughout the entire nervous system (Hobert, 2016), yet we understand little about how their expression is induced in the embryo (Baumeister et al., 1996; Bertrand and Hobert, 2009; Christensen et al., 2020; Mitani et al., 1993; Murgan et al., 2015). Based on a previously reported effect of *lin-32* on the expression of the terminal selectors *unc-86/Brn3* (Baumeister et al., 1996) and *mec-3* (Mitani et al., 1993), we sought to investigate the role of *lin-32* further. In a number of different organisms, from flies to worms to vertebrates, Atonal orthologs have mostly been characterized for their proneural activity that imposes neuronal identity on neuroectodermal progenitor cells (Baker and Brown, 2018; Bertrand et al., 2002). Loss of such proneural activity results in conversion from a neuronal to an ectodermal skin cell fate. Such proneural functions have been defined for *lin-32* in the context of a number of peripheral sense organs in *C. elegans*, including the postdeirid, Q and male ray lineages (Chalfie and Au, 1989; Portman and Emmons, 2000; Zhao and Emmons, 1995; Zhu et al., 2014). These proneural functions are evidenced by lineage changes in which neuroblasts that normally divide to generate multiple distinct neuron types instead convert to skin cells, leading to a failure to generate a number of neuron types (Chalfie and Au, 1989; Portman and Emmons, 2000; Zhao and Emmons, 1995; Zhu et al., 2014). However, other effects on neural lineages have also been observed in *lin-32* mutants. For example, after its proneural role early during lineage specification *lin-32* has also been implicated in controlling later aspects of neuronal differentiation in the Q and ray lineages (Miller and Portman, 2011; Portman and Emmons, 2000; Zhu et al., 2014). Cell identity transformations are also evident in a subset of dopaminergic neuron-producing lineages (Doitsidou et al., 2008) as well as in glia cells (Zhang et al., 2020). *lin-32* has also been shown to affect the differentiation and/or function of a number of additional neuron types, including oxygen sensory neurons (Rojo Romanos et al., 2017), touch receptor neurons (Mitani et al., 1993), anterior ganglion neurons (Baumeister et al., 1996; Shaham and Bargmann, 2002) and AIB interneurons (Hori et al., 2018). However, it was left unclear whether these defects are proneural lineage defects, cellular differentiation defects, cell identity transformation defects or some combination thereof.

Here, to facilitate a comprehensive analysis of *lin-32* function, we begin by describing the expression pattern of *gfp*-tagged LIN-32. Although the expression of *lin-32::gfp* is consistent with a number of previously described functions of *lin-32*, we identified sites of expression that led us to explore previously unknown functions of *lin-32*. One consistent theme of *lin-32* function is its effect on the expression of terminal selector-type transcription factors. Our findings for *lin-32*, as well as for another bHLH family of the Atonal superfamily, *hlh-14*, provide insights into the molecular basis for the convergence of distinct lineage histories on similar cellular differentiation events, via the regulation of terminal selector expression.

RESULTS

Embryonic expression pattern of *lin-32*

The embryonic expression of *lin-32* has so far only been described using a 5′ promoter fusion, which may lack *cis*-regulatory elements (Murray et al., 2012). We analyzed a transgenic strain carrying a fosmid in which the *lin-32* locus was 3′-terminally tagged with *gfp*, as well as a CRISPR/Cas9-engineered reporter allele in which *gfp* was also inserted at the 3′ end of the gene (kindly provided by the Greenwald lab, Columbia University, NY, USA), both of which yielded similar expression patterns. Embryonic expression was analyzed using 4D microscopy (Schnabel et al., 1997). We focused on the AB blastomere- and MS blastomere-derived lineages, which produce all but two (PVR and DVC) of the 302 neurons of the *C. elegans* nervous system. We found that *lin-32* was expressed in a number of different neuronal lineages in the AB lineage, but not the MS lineage, which produces several pharyngeal neurons (Fig. 1). The earliest expression was observed at the 128-cell stage in the daughters of ABalapa blast cells. In other lineages, the onset of *lin-32* expression occurred shortly after the 128-cell stage, whereas, elsewhere, it started as late as a mother neuroblast, which generates two terminally differentiating daughters. In several cases, we were unable to record the terminal division of a neuroblast because of the movement of embryos in the egg shell and, therefore, we may have missed expression in postmitotic cells. If postmitotic expression were to exist, it would be transient because we observed no expression of *lin-32* in any embryonically generated neuron in first larval or later-stage animals. This fosmid reporter-based expression is largely similar to that of the promoter fusion (Murray et al., 2012), but pushes that expression pattern to one additional round of cell cleavage.

Consistent with the expression of Atonal homologs in other organisms (Bertrand et al., 2002; Jarman and Groves, 2013), the vast majority of lineages that expressed *lin-32* produced sensory neurons. Several aspects of the embryonic expression of *lin-32* were in agreement with previously reported *lin-32* mutant phenotypes. For example, we observed *lin-32* expression (Fig. 1) in lineages that give rise to sensory neurons in the anterior ganglion, consistent with previous studies that reported *lin-32* to control expression of the *unc-86/Brn3* terminal selector (Baumeister et al., 1996; Shaham and Bargmann, 2002). Similarly, we observed expression in lineages that give rise to URX and CEPD neurons, and in lineages that give rise to AIB neurons, which are all neurons wherein differentiation defects have been observed in *lin-32* mutants (Doitsidou et al., 2008; Hori et al., 2018; Rojo Romanos et al., 2017).

Proneural functions of *lin-32*

Previous work had shown that *lin-32* has proneural functions in a number of postembryonically generated sensory neuronal cell types, including the sex-shared postdeirid lineage and the Q lineage, as well as in male-specific neuronal lineages (Chalfie and Au, 1989; Portman and Emmons, 2000; Zhao and Emmons, 1995). One common feature in these postembryonic lineages appears to be that the loss of *lin-32* results in obvious lineage-patterning defects, in which neuroblasts stop dividing and transform into hypodermal cells. The embryonic expression of *lin-32* that we described above prompted us to ask whether such neuroblast-to-hypodermal conversions are also observed in embryonically generated neurons of *lin-32*-null mutant animals (i.e. carrying the *tm1449* deletion allele; Fig. 1). Nomarski optics-based lineage tracing of embryonic cell lineages was performed using 4D microscopy with SIMI BioCell (Schnabel et al., 1997) until 300 min of embryonic development. This analysis revealed no obvious cell-division defects or transformations into hypodermal fates (as would be

Development (2021) 148, dev199224. doi:10.1242/dev.199224

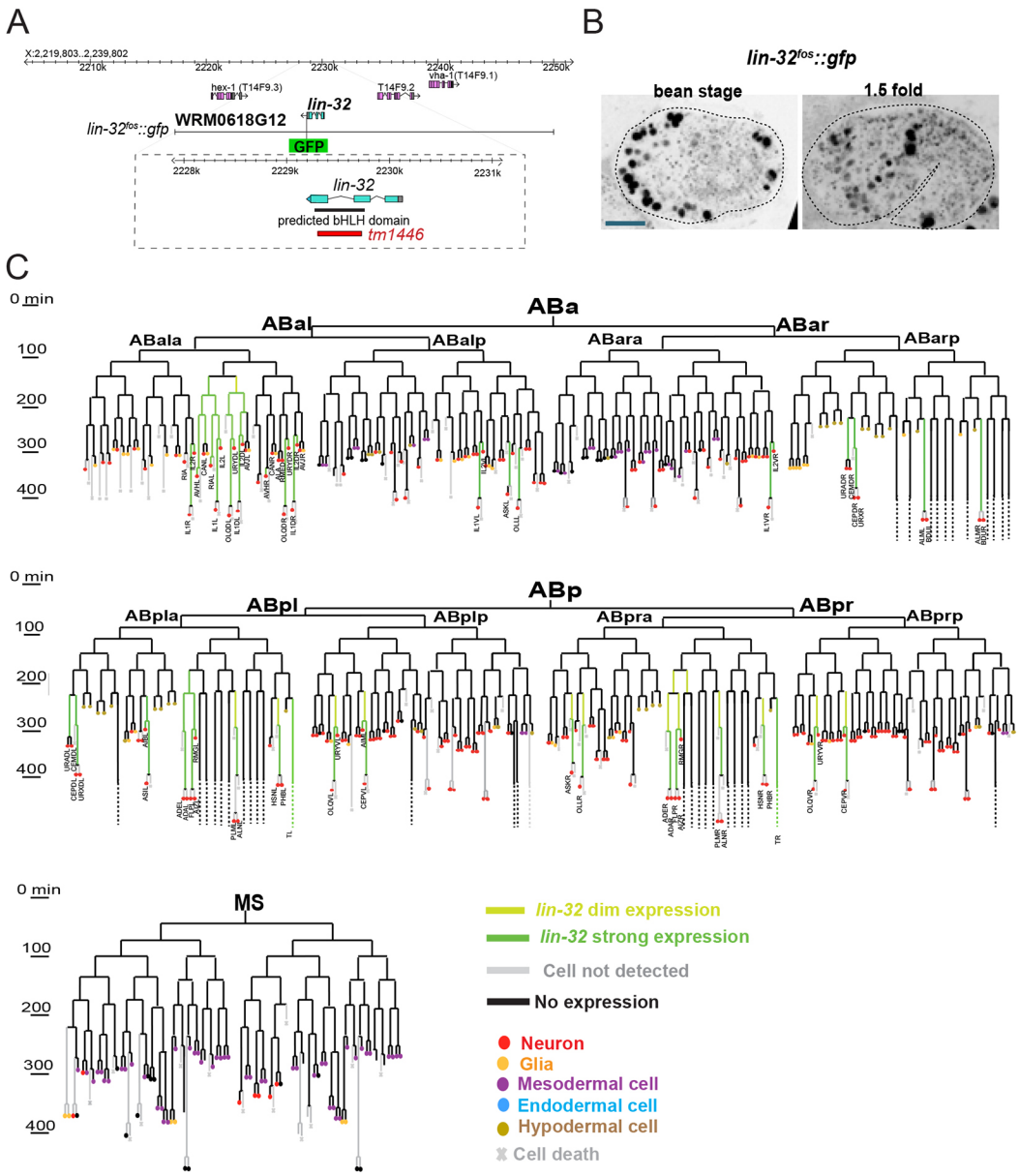

Fig. 1. *lin-32* expression pattern. (A) Schematic of gene structure, showing removal of the bHLH domain from the *lin-32* locus by the deletion allele *tm1664* and reporter genes. (B) Representative images of *lin-32* fosmid gene expression (*otIs594*) at embryonic stages when most terminal neurons are born. Dashed outlines indicate embryo shape. (C) *lin-32* fosmid expression (*otIs594*) in the AB and MS lineages, which produce all but two of the 118 neuron classes of the hermaphrodite. The *lin-32* fosmid reporter is first detected shortly after 100 min into development in ABalap descendants. Our analysis revealed that *lin-32::gfp* is expressed in both mitotically active neuroblasts during embryogenesis and a subset of postmitotic neurons. Scale bar: 10 µm.

evidenced by changes in nuclear morphology and migratory patterns) in any of the lineages that normally express *lin-32*.

For a more granular assessment of cell fate, we examined the expression of different sets of pan-neuronal cell-fate markers. First, we used a nuclear-localized reporter transgene for the pan-neuronal gene *rab-3* (Stefanakis et al., 2015). We counted the number of nuclei and, with the exception of the ventral nerve cord, observed a reduction in overall pan-neuronal gene expression throughout embryonically generated head and tail ganglia (Fig. 2A). To confirm this observation, we used the 'UPN' driver hybrid reporter construct, in which the *cis*-regulatory elements of several pan-neuronally expressed genes are fused with one another (Yemini et al., 2021). We observed that expression of this pan-neuronal marker gene was also lost in many different normally *lin-32*-expressing lineages (Fig. 2B, Fig. 3). Lastly, we also examined the existence of subnuclear granules ('NUN bodies'), another pan-neuronal identity feature (Pham et al., 2021), observing a reduction in the number of cells containing this subnuclear structure (Fig. 2C).

The hybrid pan-neuronal marker was expressed from the recently described NeuroPAL transgene, which also contains a large number of additional neuron type-specific markers (Yemini et al., 2021). These markers allowed us to assess more specifically which neurons lose their identity and to correlate these losses with normal sites of *lin-32* expression. We observed pan-neuronal and cell type-specific marker losses in AIB and URX neurons, which were previously reported to display differentiation defects in *lin-32* mutants (Hori et al., 2018; Rojo Romanos et al., 2017) (Fig. 3). Within the anterior ganglion, we observed losses of pan-neuronal and cell-specific

Development (2021) 148, dev199224. doi:10.1242/dev.199224

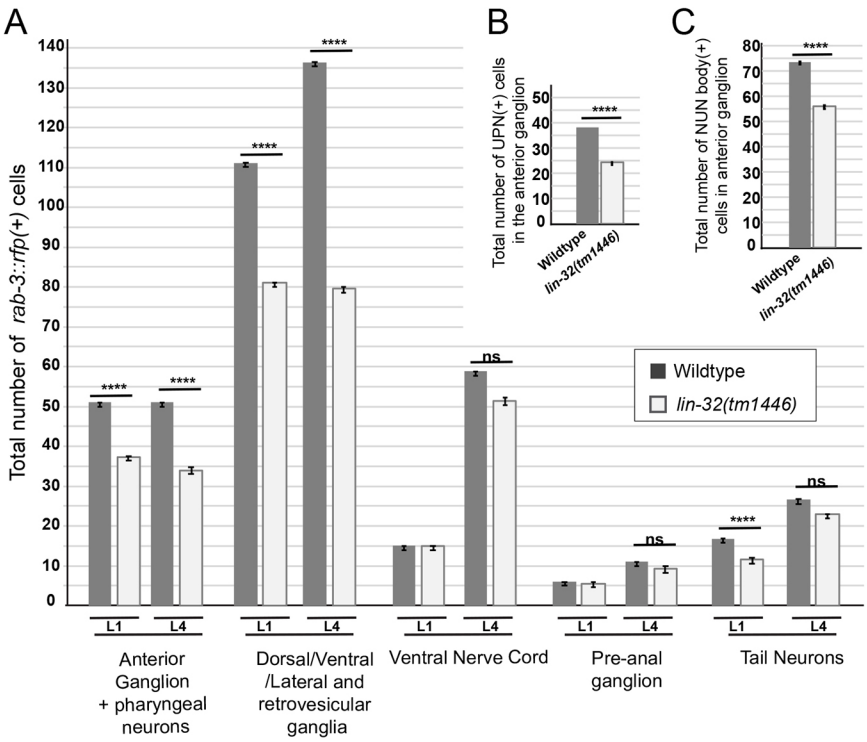

Fig. 2. Proneural activities of *lin-32* throughout the animal. (A) Total number of cells expressing the *rab-3* marker *otIs356*. Expression of the pan-neuronal gene *rab-3* is affected in different ganglia of the *lin-32*-null mutant (n=25). (B) The total number of cells expressing the UPN pan-neuronal marker (contained within the NeuroPAL transgene *otIs669*). The UPN reporter consists of four pan-neuronal promoters from the *ric-19*, *rgef-1*, *unc-11* and *ehs-1* loci (Yemini et al., 2021). We only scored UPN in the anterior ganglion (n=30). (C) The total number of cells with speckled subnuclear morphology ('NUN bodies') was scored in the anterior ganglion, using Nomarski optics (n=30). All graphs show mean±s.e.m. ****P <0.0001 (two-way ANOVA with Tukey test for correction of multiple comparisons). ns, not significant.

markers of the radially symmetric IL1 and IL2 sensory neuron classes, consistent with *lin-32* expression in the lineages that generate these neurons. We independently corroborated the IL1 and IL2 neuron losses with different marker transgenes (*klp-6* for IL2 and *flp-3* for IL1) (Fig. S2).

In a previous screen for mutants that affect dopaminergic cell fate, we had identified alleles of *lin-32* and reported that *lin-32* affects the expression of the dopaminergic marker *dat-1::gfp* in CEPD neurons (Doitsidou et al., 2008). Here, we found that *lin-32* is expressed in the lineage that gives rise to CEPD neurons. Using NeuroPAL, we showed that *lin-32* affects expression of not only the *dat-1* marker, but also other cell-identity markers, in addition to pan-neuronal gene expression in CEPD neurons. These results indicate that *lin-32* also acts as proneural factor in this lineage (Fig. 3).

lin-32 is required for terminal selector expression

To examine the nature of these differentiation defects further, we asked whether *lin-32* controls the expression of the terminal selector-type transcription factors known to specify the identity of the neurons affected by *lin-32* (Hobert, 2016). We found that the expression of *unc-86*, the identity regulator of IL2 and URX neurons (Shaham and Bargmann, 2002; Zhang et al., 2014), is indeed lost in *lin-32* mutants (Fig. 4). Expression of *ceh-43/Dlx* and *ceh-32/Six3*, candidate terminal selectors for IL1 neurons (Reilly et al., 2020), and expression of *lin-11/Lhx1*, a candidate terminal selector for AVJ neurons, was affected in their respective neurons (Fig. 4). Similarly, expression of *ceh-43*, the terminal selector for CEPD neurons (Doitsidou et al., 2013), was lost in CEPD neurons of *lin-32* mutants (Fig. 4), consistent with the loss of terminal CEPD identity markers in *lin-32* mutants (Fig. 3) (Doitsidou et al., 2008), and expression of the AIB identity regulator *unc-42* (Bhattacharya et al., 2019), was affected in AIB neurons (Fig. 3).

Given that terminal selectors, such as *unc-86*, *unc-42* and *ceh-43*, do not affect pan-neuronal gene expression (Berghoff et al., 2021; Bhattacharya et al., 2019; Doitsidou et al., 2013; Hobert, 2016), we conclude that *lin-32* independently regulates two aspects of the neuronal differentiation programs of cells such as IL2, IL1 or AIB neurons: (1) pan-neuronal identity; and (2) the acquisition of neuron type-specific features via regulation of terminal-selector transcription factors.

lin-32 affects terminal identity markers in subsets of neuronal class members

The effect of *lin-32* on a number of different neuron classes reveals an interesting phenomenon. All six IL2 class members are very similar neurons based on process projection patterns, synaptic connectivity (White et al., 1986) and molecular markers (Taylor et al., 2020 preprint), and their common identity is specified by the terminal selectors *unc-86*, *sox-2* and *cfi-1* (Shaham and Bargmann, 2002; Vidal et al., 2015; Zhang et al., 2014). However, we found that loss of *lin-32* affected the differentiation of the dorsal and lateral IL2 pairs more extensively than the ventral IL2 pairs (Figs 3 and 4). The subclass-selective effect of *lin-32* correlates with the intriguing phenomenon that all six IL2 neurons derive from distinct lineages yet converge on the same neuron type. The dorsal and lateral IL2 pairs are all generated within the ABala lineage branch, whereas the ventral pairs are generated by the lineally distal ABalpp and ABarap branch (Fig. 1). In the ABala branch, where loss of *lin-32* shows an effect, *lin-32* is normally expressed early in the lineage, whereas, in the branches that produce the ventral pairs in a *lin-32*-independent manner, *lin-32* is expressed much later (Fig. 1).

Another case of subclass-specific expression defects was observed in the dopaminergic CEP neuron class, composed of a dorsal pair (CEPDL/R) and a ventral pair (CEPDVL/R). These two pairs are anatomically very similar (White et al., 1986) and, in the terminally differentiated state, molecularly indistinguishable (Taylor et al., 2021). However, each pair derives from distinct embryonic neuroblasts (Fig. 1). As described above, we found that *lin-32* has a proneural function in CEPD neurons (Fig. 3). However, even though *lin-32* is expressed in CEPV neurons (albeit much later

Development (2021) 148, dev199224. doi:10.1242/dev.199224

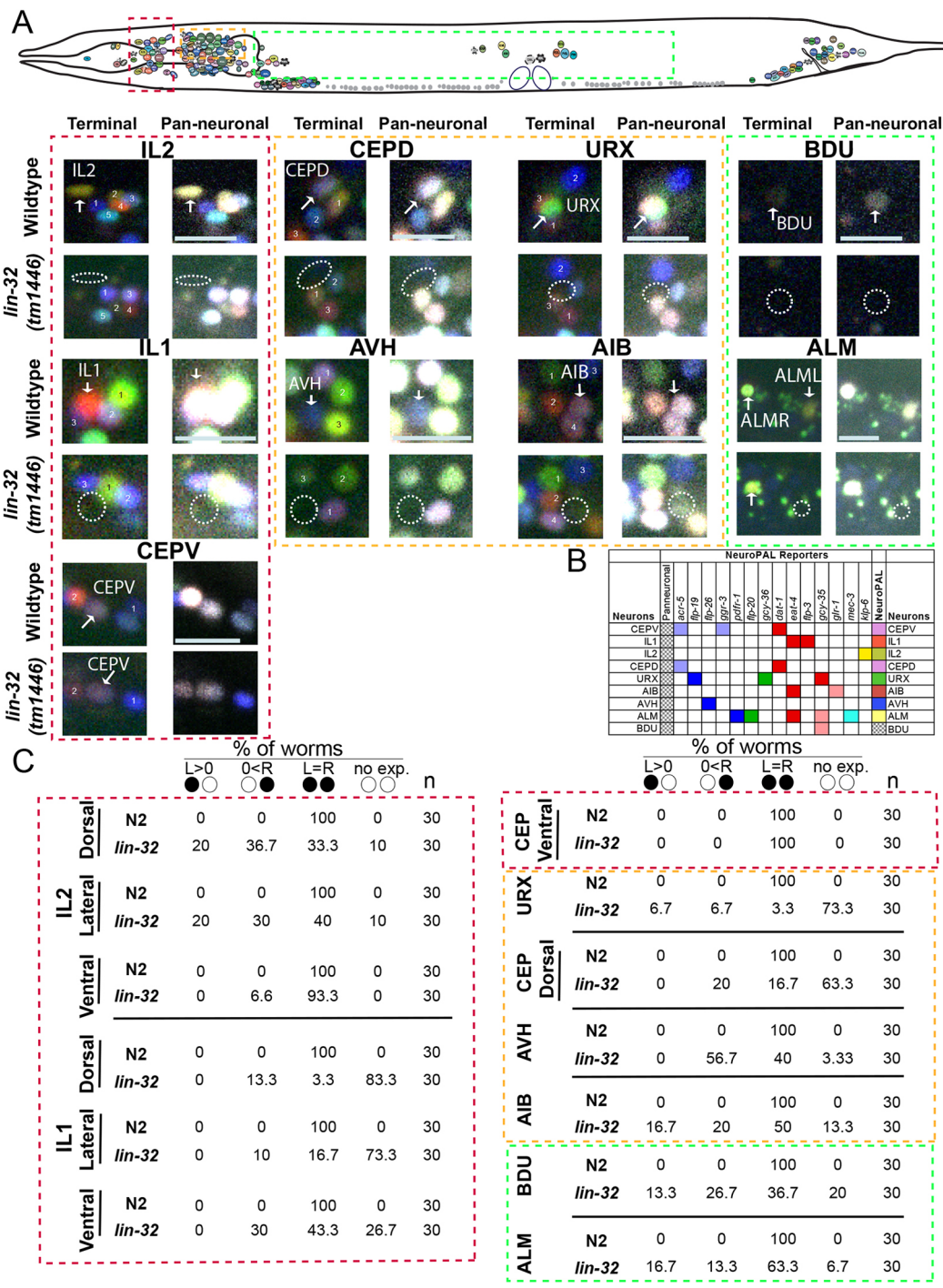

		L>0	0<R	L=R	no exp.	n
IL2 Dorsal	N2	0	0	100	0	30
	lin-32	20	36.7	33.3	10	30
IL2 Lateral	N2	0	0	100	0	30
	lin-32	20	30	40	10	30
IL2 Ventral	N2	0	0	100	0	30
	lin-32	0	6.6	93.3	0	30
IL1 Dorsal	N2	0	0	100	0	30
	lin-32	0	13.3	3.3	83.3	30
IL1 Lateral	N2	0	0	100	0	30
	lin-32	0	10	16.7	73.3	30
IL1 Ventral	N2	0	0	100	0	30
	lin-32	0	30	43.3	26.7	30
CEP Ventral	N2	0	0	100	0	30
	lin-32	0	0	100	0	30
URX	N2	0	0	100	0	30
	lin-32	6.7	6.7	3.3	73.3	30
CEP Dorsal	N2	0	0	100	0	30
	lin-32	0	20	16.7	63.3	30
AVH	N2	0	0	100	0	30
	lin-32	0	56.7	40	3.33	30
AIB	N2	0	0	100	0	30
	lin-32	16.7	20	50	13.3	30
BDU	N2	0	0	100	0	30
	lin-32	13.3	26.7	36.7	20	30
ALM	N2	0	0	100	0	30
	lin-32	16.7	13.3	63.3	6.7	30

Fig. 3. Proneuronal activities of *lin-32* in specific lineages. (A) The terminal, neuron type-specific and pan-neuronal identities of many neurons that express *lin-32* during development are affected in *lin-32(tm1446)*, as revealed here using the cell-fate marker strain NeuroPAL (*otIs669*). Boxes with different color codes highlight the ganglia for neurons (schematized at the top of the figure) exhibiting fate defects. Neurons (indicated by 1, 2, 3, etc.) that differ in wild-type versus mutant animals are indicated by arrows (see Materials and Methods for notes on cell identification); the locations where neuron colors are missing from mutants are circled by a dashed line. Neighboring neurons with similar identity in mutant and wild-type animals are labeled with corresponding numbers (some neuron colors appear to differ between wild type and mutant because some neurons lie out of the plane of focus; see Materials and Methods and Fig. S1). The neighboring neurons are used as landmarks to ID the cell of interest (see Materials and Methods). (B) The NeuroPAL reporter-fluorophore combinations that were responsible for coloring each neuron type. Cell-fate alterations are determined by changes in this color code. With this code, lost colors can be directly mapped back to losses of reporter expression, thereby determining mutant effects on cell identity. (C) Data for the terminal and pan-neuronal fate defects shown in A, indicating the percentage of animals that display the wild-type NeuroPAL color code for the indicated neuron class. No instances were observed in which the terminal markers were affected but the pan-neuronal identity remained intact. The same effects of *lin-32* on *dat-1* expression in CEPD (i.e. loss of expression) and CEPV (i.e. no effect detected) have been previously reported (Doitsidou et al., 2008). Circles indicate bilateral left-right homologs of the respective neuron class (L>0, expression only in left neuron; 0<R, expression only in right neuron; L=R, expression in both neurons, i.e. wild type). Scale bars: 10 µm.

Development (2021) 148, dev199224. doi:10.1242/dev.199224

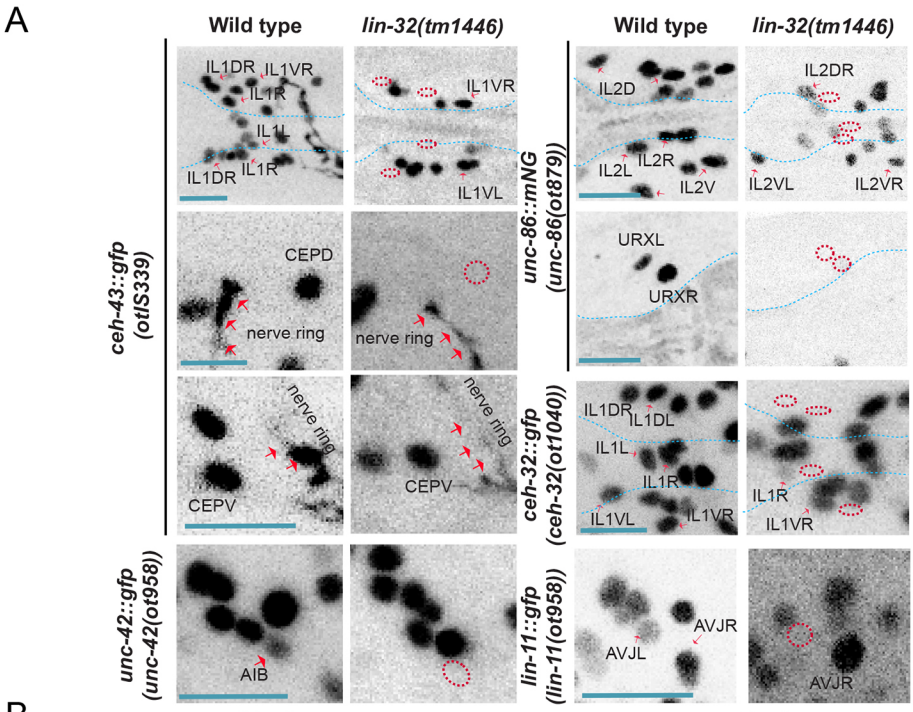

B

% of worms

				L>0 ●○	0<R ○●	L=R ●●	no exp. ○○	n
ceh-43::gfp	IL1	Dorsal	N2	0	0	100	0	30
			lin-32	0	0	0	100	20
		Lateral	N2	0	0	100	0	30
			lin-32	0	0	25	75	20
		Ventral	N2	0	0	100	0	30
			lin-32	0	15	10	75	20
	CEP	Dorsal	N2	0	0	100	0	30
			lin-32	0	0	0	100	20
		Ventral	N2	0	0	100	0	30
			lin-32	0	0	100	0	20
unc-42::gfp	AIB		N2	0	0	100	0	25
			lin-32	17.4	21.7	52.2	8.7	23
lin-11::gfp	AVJ		N2	0	0	100	0	30
			lin-32	10	20	70	0	20

% of worms

				L>0 ●○	0<R ○●	L=R ●●	no exp. ○○	n
unc-86::mNG	IL2	Dorsal	N2	0	0	100	0	30
			lin-32	20	35	35	10	20
		Lateral	N2	0	0	100	0	30
			lin-32	20	40	30	10	20
		Ventral	N2	0	0	100	0	30
			lin-32	0	10	90	0	20
	URX		N2	0	0	100	0	30
			lin-32	0	0	0	100	20
ceh-32::gfp	IL1	Dorsal	N2	0	0	100	0	30
			lin-32	0	0	0	100	20
		Lateral	N2	0	0	100	0	30
			lin-32	0	40	0	60	20
		Ventral	N2	0	0	100	0	30
			lin-32	0	70	30	0	20

Fig. 4. Effect of *lin-32* on the expression of candidate terminal selectors. (A,B) Loss of candidate terminal selector expression in *lin-32(tm1446)*-null mutants. Reporters were: *lin-11[ot958(lin-11::gfp::FLAG)]*, *ceh-32[ot1040(ceh-32::gfp)]*, *unc-86[ot879(unc-86::nNeonGreen)]*, *otIs339 (ceh-43^{fosmid}::gfp)* and *unc-42 [ot958(unc-42::gfp)]*. (A) Representative images of wild-type and mutant phenotypes; red dashed outlines indicate location of the defective cell; blue dashed outlines indicate outline of pharynx; red arrows indicate nerve ring. (B) Percentage of animals that displayed indicated marker gene defect in the left (L) or right (R) neuron of a bilateral neuron pair. NeuroPAL (*otIs696*) was used in the background of all of the strains mentioned herein in order to identify neurons expressing the terminal selector. Circles indicate bilateral homologs of the respective neuron class (L>0: expression only in left neuron; 0<R: expression only in right neuron; L=R: expression in both neurons, i.e. wild type). Scale bars: 10 µm.

than in the CEPD neuron-producing lineage; Fig. 1), we detected no defect in the generation or differentiation of CEPV neurons in *lin-32*-null mutants. Pan-neuronal marker expression and terminal identity markers were unaffected (Fig. 3), as was expression of the terminal selector *ceh-43* (Fig. 4).

Strikingly, *lin-32* also selectively affects lineally convergent neuron class members in left/right symmetric neuron class members. Within the ABala lineage branch, the left and right AVH neurons are generated from two nonsymmetric precursor cells: ABalapaaa (giving rise to AVHL) and ABalappap (giving rise to AVHR) (Fig. 5A). Another neuron pair generated by these two different blast cells are the left CAN (CANL) and the right CAN (CANR) neurons (Fig. 5A). Similar to the six IL2 neurons, each of these two left/right symmetric neurons pairs is again an example of lineage convergence, where nonbilaterally symmetric lineage histories funnel into the generation of indistinguishable left/right neuron pairs. We observed that *lin-32* was expressed in a left/right asymmetric manner in the lineages that give rise to AVHL/R and CANL/R neurons. In the lineage branch that gives rise to the left AVH and the left CAN, *lin-32* was expressed throughout the lineage, whereas it was expressed only very late in the postmitotic AVHR and not at all in CANR or the lineage that gives rise to it (Fig. 5). As stated above, we observed that *lin-32* did not affect the cellular cleavage pattern that gives rise to these cell types. However, we discovered that loss of *lin-32* affected, in a left/right

Development (2021) 148, dev199224. doi:10.1242/dev.199224

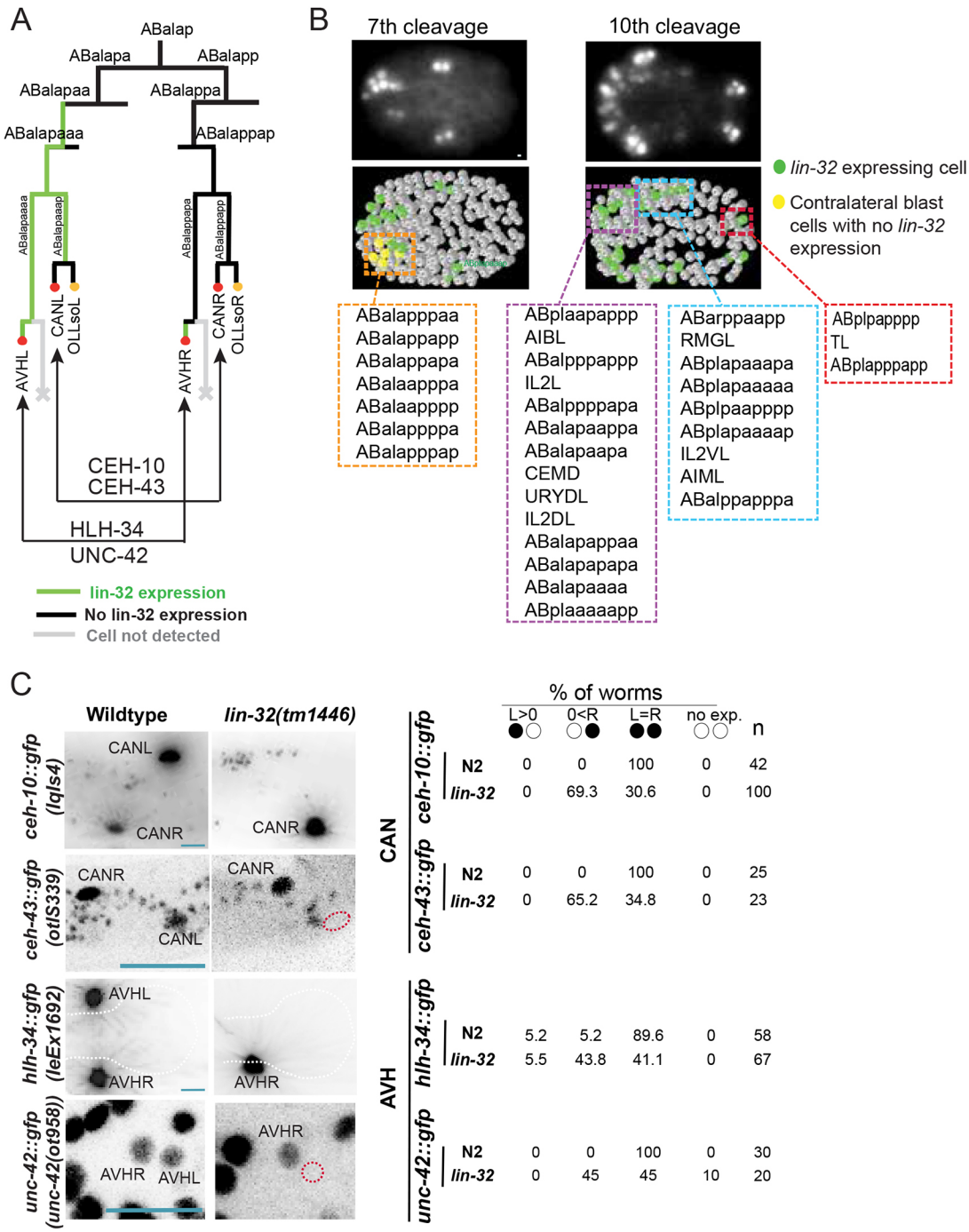

Fig. 5. Left/right asymmetric neuronal defects in *lin-32* mutants. (A) ABalapa descendants are the first blast cells to show expression of *lin-32*. The ABalapa lineage gives birth to two neurons, AVHL and CANL, among many others (red circle, neuron; yellow circle, glia). Conversely, their right contralateral homologs derive from the ABalapp lineage, which expresses *lin-32* later and more selectively. (B) Representative images of *lin-32* gene expression in the 7th (mitotically active cells) and 10th (postmitotic cells) cleavage stages. The lower panels show the ball models for the same embryonic stages shown in the images in the upper panels. Color-coded boxes represent different regions of the embryo. The names of the terminal and blast cells are indicated in the color-coded boxes. (C) The effect of *lin-32(tm1446)* was determined using terminal selector reporters for AVH and CAN (left images); *lin-32* is asymmetrically expressed in the ancestors of these neurons. The red-dashed outlines indicate the position of cells with defects; the white-dashed lines indicate outline of pharynx. The percentage of animals that displayed respective reporter gene expression is shown on the right. Circles indicate bilateral homologs of the respective neuron class (L>0: expression only in left neuron; 0<R: expression only in right neuron; L=R: expression in both neurons, i.e. wild type). Scale bar: 10 µm.

asymmetric manner, the expression of terminal selector-type transcription factors that define the molecular identity of neuron pairs within the ABala lineage. Specifically, *lin-32* affected the expression of *unc-42* and *hlh-34*, the joint identity regulators of the AVH neuron class (Berghoff et al., 2021), in only the left AVH neuron (AVHL), where *lin-32* expression begins as early as the great-grandmother of AVHL, but not in the right AVH neuron (AVHR), where we observed no *lin-32* expression (Fig. 5A,B).

Development (2021) 148, dev199224. doi:10.1242/dev.199224

The same left/right symmetric effect was observed in the CAN neuron pair. CANL/R identity is specified by the Prd-type homeobox gene (Forrester et al., 1998; Wenick and Hobert, 2004) and may operate together with the Distal-less ortholog *ceh-43* (Reilly et al., 2020). We found that *lin-32* affects expression of the CANL/R identity regulator *ceh-10* as well as its candidate co-factor *ceh-43/Dlx* in CANL, but not in CANR (Fig. 5C).

The Achaete-Scute homolog *hlh-14* provides a mirror image of *lin-32* function

We considered the possibility that another bHLH transcription factor may provide a mirror-image function of *lin-32* in controlling the identity of neurons that are contralateral to those affected by *lin-32*. Unlike *Drosophila* or vertebrates, *C. elegans* only encodes a single Atonal ortholog (Baker and Brown, 2018; Zhao and Emmons, 1995). The next closely related bHLH genes are *ngn-1* and *cnd-1*, the single Neurogenin and NeuroD orthologs of *C. elegans* that, together with Atonal, form the Ato superfamily of bHLH genes (Hallam et al., 2000; Hassan and Bellen, 2000; Nakano et al., 2010). To examine their expression throughout all stages of embryonic and postembryonic development of the hermaphrodite, we generated a strain with a fosmid reporter transgene for *cnd-1* and used a previously described *ngn-1* reporter transgene that contains the entire *ngn-1* locus and is capable of rescuing *ngn-1* mutant phenotypes (Nakano et al., 2010). We again focused on the AB and MS lineages, which produce all but two of the 118 neuron classes. Each gene was selectively expressed in multiple neuronal lineages, with *ngn-1* being expressed in more lineages compared with *cnd-1* (Fig. S3). Expression was always transient (i.e. it did not endure in any neuron into postembryonic stages). *ngn-1* and *cnd-1* expression was largely non-overlapping, with the exception of the ABarapp lineage, where the expression of both genes overlapped (Fig. S3). Compared with *lin-32* expression, we observed no asymmetric expression within bilaterally symmetric neuron pairs in the ABala lineage that mirrored the asymmetric expression of *lin-32*.

As the next gene candidates, we considered the expression patterns of four homologs of the *Drosophila* Achaete-Scute complex (AS-C): *hlh-6*, *hlh-19*, *hlh-3* and *hlh-14*. Their expression patterns had not previously been reported throughout the embryonic nervous system. A fosmid-based *hlh-6* reporter was exclusively expressed in pharyngeal gland cells, as previously reported with smaller reporters (Smit et al., 2008). We used CRISPR/Cas9 to tag endogenous *hlh-19* with *gfp* and observed no expression at any stage of embryonic development. In contrast, a *hlh-3* fosmid-based reporter, as well as a CRISPR-generated reporter allele (kindly provided by N. Flames, IBV, Valencia, Spain), showed widespread expression throughout the developing embryonic nervous system (Fig. 6). The *hlh-14* fosmid reporter also showed embryonic expression in neuronal lineages, but its expression was more restricted (Fig. 6). Intriguingly, in the context of the ABalap lineage, where we observed left/right asymmetric *lin-32* expression (Fig. 1), we observed that *hlh-14* (but not *hlh-3*) displayed a mirror-image asymmetry of this expression. In those left/right symmetric lineages where we observed differential later expression of *lin-32*, we observed differential earlier expression of *hlh-14*, and vice versa (Fig. 7A-C).

To assess the functional significance of this expression, we examined two different left/right symmetric neuron pairs, CANL/R and AVHL/R, in *hlh-14*-null mutants. We observed mirror-image defects in *hlh-14* mutants: CANR, but not CANL, showed defects in *ceh-10* expression (the opposite phenotype to *lin-32*), and AVHR, but not AVHL, showed defects in *hlh-34* expression (also the opposite phenotype to *lin-32*) (Fig. 7D). We further note that *hlh-14* was also expressed as a mirror image in other lineages, particularly the IL1 and IL2 lineages, where *lin-32* showed differential expression in individual class members.

Neuronal identity transformations in *lin-32* mutants

Returning to our original analysis of *lin-32* mutants, we considered cases in which we observed expression of *lin-32*, but no apparent loss of neuronal identity upon loss of *lin-32*. One example is the anterior deirid lineage, which produces a group of five bilaterally symmetric neuron pairs (ADE, ADA, AIZ, FLP and RMG) and expresses *lin-32* early and uniformly (Fig. 8A). We detected no proneural functions of *lin-32* (i.e. no loss of the pan-neuronal marker) and no obvious defects of the cellular cleavage pattern in this lineage. A marker (*dat-1::gfp*) expressed in one neuron class in the lineage, the dopaminergic ADE neuron, is expressed in several additional cells in *lin-32* mutants (Doitsidou et al., 2008), but it had been unclear whether these cells are ectopically generated cells or whether the marker is aberrantly expressed in other cells of this lineage. The use of the NeuroPAL transgene (Yemini et al., 2021), which provides unique labels to all cells in the lineage, provided us with the opportunity to assess this defect in more detail. We independently confirmed the ectopic dopamine marker gene expression and found that it was paralleled by a loss of expression of markers for the AIZ, ADA, FLP and RMG neurons (Fig. 8B,D). Hence, AIZ, ADA, FLP and RMG appear to have transformed their identity to that of ADE neurons.

All of the four neuron classes that transformed to ADE identity in *lin-32* mutants normally express the *unc-86/Brn3* POU homeobox gene (Finney and Ruvkun, 1990; Serrano-Saiz et al., 2018) (Fig. 8A). *unc-86/Brn3* acts as a terminal selector in at least one of these neurons, FLP (Topalidou and Chalfie, 2011), and perhaps others as well (Serrano-Saiz et al., 2013). Therefore, we tested whether loss of *lin-32* function affects *unc-86* expression in these cells. Using an *mNeonGreen*-tagged *unc-86* locus as a reporter for *unc-86* expression (Serrano-Saiz et al., 2018), we indeed observed a loss of *unc-86* expression in all four neuron classes of the lineage (Fig. 8E). A similar result was also described previously using an antimorphic allele of *lin-32*, *u282* (Baumeister et al., 1996). Future work will determine whether the neuronal identity transformations observed in *lin-32* mutants in the anterior deirid lineage are explained entirely by the loss of *unc-86* expression.

We observed another cell identity transformation in *lin-32* mutant lineages that generate the four radially symmetric OLQ and URY neurons (Fig. 9A). These neurons derive from four neuroblasts: ABalapapap, ABalapppap, and the two bilaterally symmetric ABp(l/r)paaappp neuroblasts. All of these neuroblasts were *lin-32* positive and maintained *lin-32* expression throughout ensuing divisions. As in the anterior deirid lineage, we found no proneural functions of *lin-32* in these lineages (i.e. we observed no obvious defects in cellular cleavage pattern in the lineage until the 300-min stage; neither did we observe loss of pan-neuronal reporter expression. Instead, we observed another apparent neuronal identity transformation: OLQ neurons lost characteristic marker gene expression and instead gained expression of URY marker genes (Fig. 9B-E). As in the anterior lineage, we sought to extend this observation by analyzing the expression of potential cell-identity regulators in this lineage. A potential URY identity regulator is the homeobox gene *ceh-32/Six3*, which is expressed in URY but not OLQ (Reilly et al., 2020). We observed that, in *lin-32* mutants, OLQ neurons gained *ceh-32/Six-3* expression (Fig. 9F). This is a situation that is conceptually similar to the anterior deirid lineage, in which lineally related cells that all

Development (2021) 148, dev199224. doi:10.1242/dev.199224

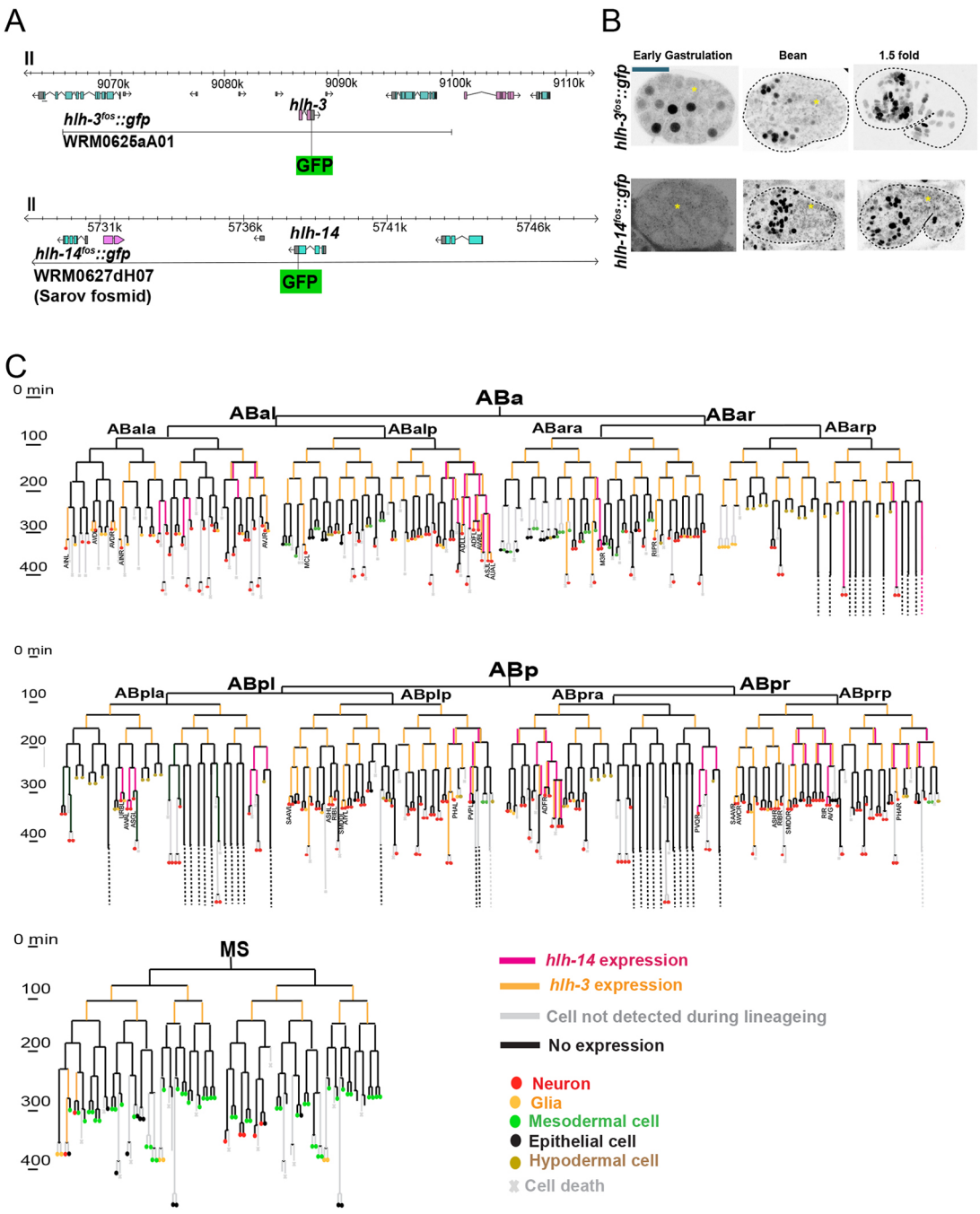

Fig. 6. Embryonic expression of the AS-C homologs *hlh-3* and *hlh-14*. (A) *hlh-3* and *hlh-14* gene structures and fosmid reporters (*otIs648* and *otIs713*, respectively) used for expression pattern analysis. (B) Representative images of *hlh-3 and hlh-14* fosmid reporters during different stages of embryonic development, showing the time when the expression starts in blast cells to the time when all postmitotic neurons are born. Yellow asterisks indicate cytoplasmic autofluorescence. (C) Lineage diagram of the expression pattern of *hlh-3* and *hlh-14* during embryogenesis. Our analysis corroborates and extends previously published expression patterns of *hlh-14* (Frank et al., 2003; Poole et al., 2011). Scale bar: 10 µm.

express *lin-32* transform their identity to that of one alternative cell type. Taken together, we conclude that *lin-32*, either directly or indirectly, regulates the expression of terminal selector-type transcription factors that play a role in promoting specific neuronal identities and suppressing alternative identities.

DISCUSSION

We found that *lin-32* acts as a proneural gene in several distinct, embryonically generated lineages, mirroring its previously described function in postembryonic development (Zhao and Emmons, 1995). One distinguishing feature of the proneural role of *lin-32* in postembryonic versus embryonic development is that, in postembryonic development, a loss of the proneural activity of *lin-32* results in a termination of neuroblast divisions and conversion of the neuroblast to that of an ectodermal skin cell (Zhao and Emmons, 1995). In contrast, during embryogenesis, we found no evidence for the loss of *lin-32* affecting cellular cleavage patterns, or obvious conversions to hypodermal fate. What we did observe was a

Development (2021) 148, dev199224. doi:10.1242/dev.199224

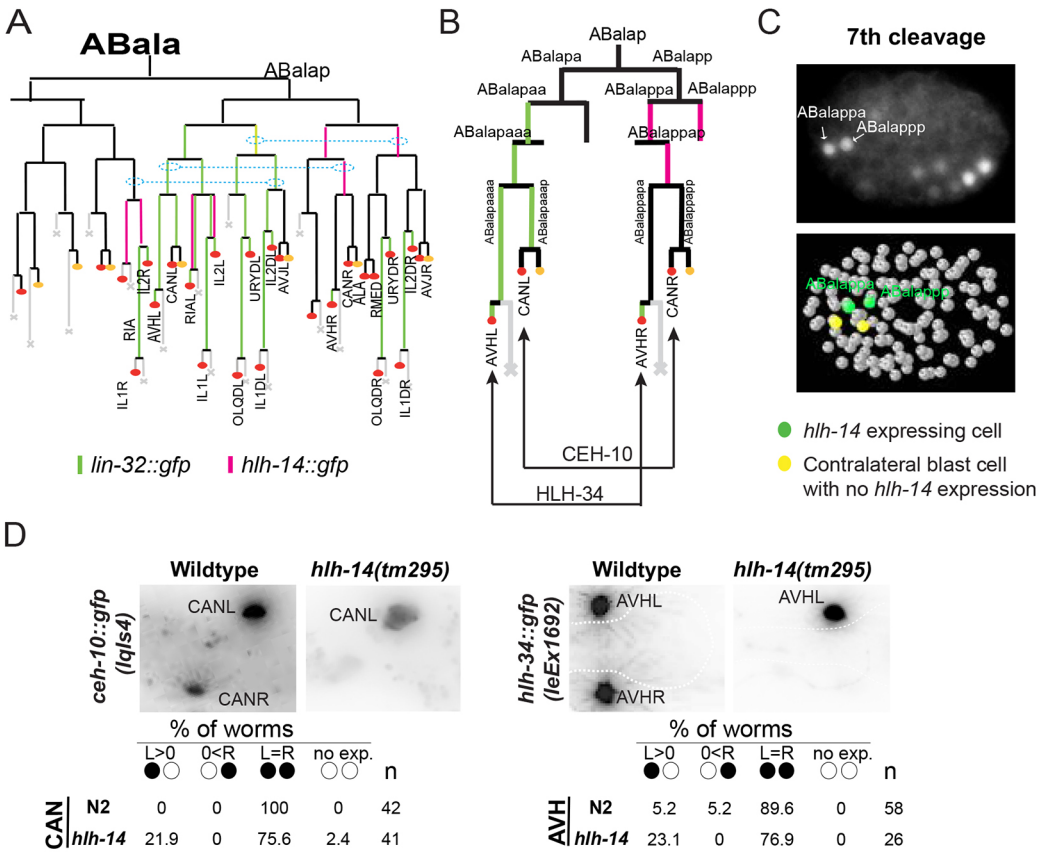

Fig. 7. Left/right asymmetric neuronal defects in *hlh-14* mutants. (A) Lineage diagram of the expression of *lin-32* and *hlh-14* fosmid reporters in the ABala lineage. *hlh-14* mirrors the expression of *lin-32* in ABalapa descendants in the ABalapp lineage. The blue dashed lines indicate sublineages that divide in a symmetric manner to produce symmetric cell fates, as shown in B. Red circle, neuron; yellow circle, glia. (B) A more focused version of the diagram in A, showing that *hlh-14* is expressed in the ABalapp descendants that give birth to AVHR and CANR, a mirror image of *lin-32* expression (see Fig. 5 in the main text). (C) Representative image of *hlh-14* gene expression at the 7th cleavage where mitotically active blast cells ABalappa/p (the great grandmother of AVHR and CANR) start expressing *hlh-14* (top panel), as also illustrated by the ball model for the same embryonic stages (bottom panel). (D) The effects of *hlh-14(tm295)* were quantified for terminal selector reporters of CAN (left) and AVH (right), as also quantified for *lin-32* mutants (also see Fig. 5C in the main text). The wild-type images are from Fig. 5C in the main text and are shown here for comparison only. The white-dashed lines indicate outline of pharynx. Circles indicate bilateral homologs of the respective neuron class (L>0: expression only in left neuron; 0<R: expression only in right neuron; L=R: expression in both neurons, i.e. wild type).

loss of expression of pan-neuronal features, a loss of cell identity-controlling transcription factors (terminal selectors) and, consequently, losses of expression of cell-specific identity features.

Our observation that *lin-32* affects the expression of terminal selectors, as well as pan-neuronal features provides support for the ‘coupling hypothesis’ of proneural gene function, proposed during the late 1990s (Brunet and Ghysen, 1999). Early studies on proneural gene function in both flies and vertebrates had shown that, whereas proneural genes affect generic neuronal features, individual bHLH genes also confer specificity to the neuronal cell type that they generate (reviewed by Baker and Brown, 2018; Bertrand et al., 2002). Brunet and Ghysen proposed that distinct proneural bHLH proteins share the ability to induce generic neuronal properties, but each have the ability to also control the expression of neuron type-specific effector genes, thereby coupling these two distinct aspects of neuronal differentiation (Brunet and Ghysen, 1999). As an example, they discussed the ability of not only the proneural mouse *Mash1* genes to activate the expression of generic neuronal features, but also the homeobox gene *Phox2* to confer specific noradrenergic traits on developing neurons (Brunet and Ghysen, 1999). Phox2 is a terminal selector of noradrenergic fate (Brunet and Pattyn, 2002; Coppola et al., 2010) and, hence, provides the first example of what we abundantly corroborate here in multiple neuronal contexts: that the proneural *lin-32* gene controls the expression of multiple distinct homeobox terminal selectors in a lineage-specific manner to specify distinct neuronal identities.

One intriguing aspect of the proneural function of *lin-32* is the highly selective and lineage-specific effect that it has on specific members of individual neuron classes. This observation provides a molecular correlate to the phenomenon of lineage convergence: cells with different lineage histories acquire similar terminal identities. Lineage convergence is widespread in the *C. elegans* nervous system (Sulston et al., 1983) and, with the advent of technologies that allow the lineages of more complex organisms to be determined, has now also been observed in vertebrates (Cao et al., 2019; Chan et al., 2019; McKenna et al., 2016; Wagner et al., 2018). In the *C. elegans* nervous system, divergent lineages of individual neuron class members converge on similar gene expression profiles via the activation of terminal selectors of neuronal identity in individual class members. For example, the six IL2 sensory neurons arise from different, nonhomologous lineages but are all specified by the combinatorial activity of three terminal selectors: *unc-86*, *cfi-1* and *sox-2* (Shaham and Bargmann, 2002; Vidal et al., 2015; Zhang et al., 2014). Likewise, the lineally diverse CEP neuron class members are all specified by the combinatorial activity of the terminal selectors *ast-1*, *ceh-43* and *ceh-20*

Development (2021) 148, dev199224. doi:10.1242/dev.199224

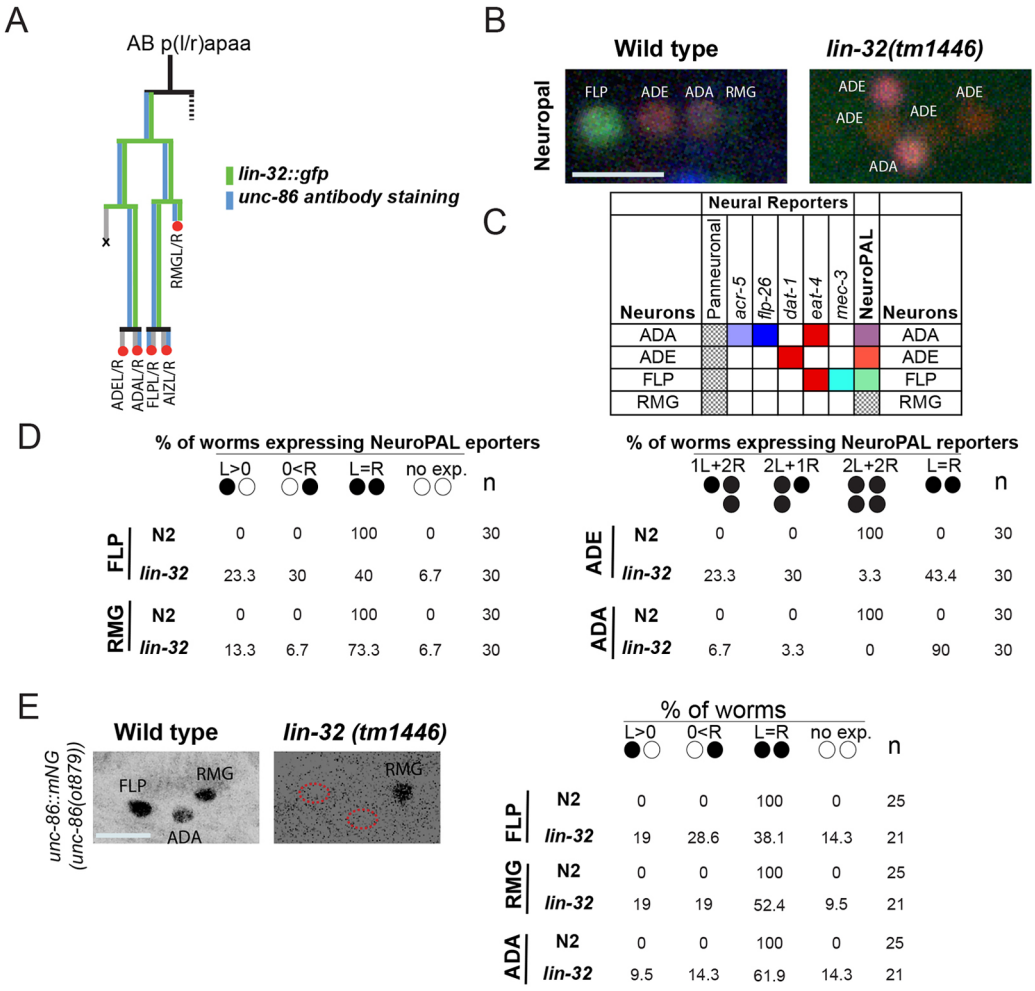

Fig. 8. *lin-32* mutants display neuronal identity fate transformation in the anterior deirid lineage. (A) Expression of *lin-32* in lineages giving birth to anterior deirid neurons. The expression of *lin-32* overlaps with the previously reported *unc-86*/*Brn3* expression (Finney and Ruvkun, 1990). The gray line indicates that we did not detect this cell during lineaging of *lin-32::gfp* expression. (B) The neuronal identities of anterior deirid neurons were observed using NeuroPAL *otIs669*. In *lin-32(tm1446)* mutants, there are ectopic neurons expressing ADE-specific terminal markers, whereas the terminal markers for FLP, RMG and sometimes for the ADA neurons are lost. (C) The combination of different reporter colors (indicated in the square) in the NeuroPAL strain used to mark cells in this lineage. (D) Percentage of different phenotypic categories observed in *lin-32(tm1446)* compared with wild type using NeuroPAL reporters. Circles indicate bilateral homologs of the respective neuron class (L>0, expression only in the left neuron; 0<R, expression only in the right neuron; L=R, expression in both neurons, i.e. wild type; 2R or 2L, expression in an additional neuron on the left or right). (E) *unc-86*/*Brn3* expression (reporter allele *ot879*) is lost in FLP, ADE and RMG neurons in *lin-32* mutants (image panels). The percentage of animals that displayed expression of the tagged *unc-86* reporter allele is shown on the right. Circles indicate bilateral homologs of the respective neuron class (L>0: expression only in left neuron; 0<R: expression only in right neuron; L=R: expression in both neurons, i.e. wild type). Scale bars: 10 µm.

(Doitsidou et al., 2013; Flames and Hobert, 2009). We have shown here that different class members are specified by distinct upstream inputs. Specifically, *lin-32* controls the generation of distinct subsets of members from a given neuron class. In the most extreme cases, we observed that the left neuron of indistinguishable bilaterally symmetric neuron classes is controlled by *lin-32*. Intriguingly, the right neuron of these neuron classes is controlled by a distinct bHLH gene, *hlh-14*. Although we have not taken our study here to the *cis*-regulatory level, it is conceivable that the *cis*-regulatory control regions of terminal selectors serve as 'integration devices' that sample distinct lineage inputs.

Apart from proneural functions in a number of different cellular contexts, we also identified roles of *lin-32* in distinguishing the execution of distinct neuronal differentiation programs, such that the loss of *lin-32* leads to a conversion of one neuronal fate to that of another neuron. We observed such homeotic identity transformations in multiple distinct lineal contexts, and we propose that these are also the result of lost terminal selector expression. Previous work has shown that, in multiple different cellular contexts, terminal selectors can act in a mutually antagonistic and competitive manner, such that removal of one selector may now enable a different selector to exert its function (Arlotta and Hobert, 2015). For example, loss of the *mec-3* homeobox gene in the ALM neuron allows UNC-86/BRN3 to pair up with a different transcription factor, PAG-3, to now promote BDU neuron fate in the ALM neuron (Gordon and Hobert, 2015; Way and Chalfie, 1988). In analogy to these cases, it is conceivable that the lost expression of some terminal selectors in *lin-32* allows other terminal selectors to promote alternative fates. For example, *unc-86/Brn3* may antagonize the expression of dopamine neuron-specifying terminal selectors in the deirid lineage and, therefore, the loss of *unc-86/Brn3* in *lin-32* mutants may lead to the induction of dopaminergic neuron fate.

Development (2021) 148, dev199224. doi:10.1242/dev.199224

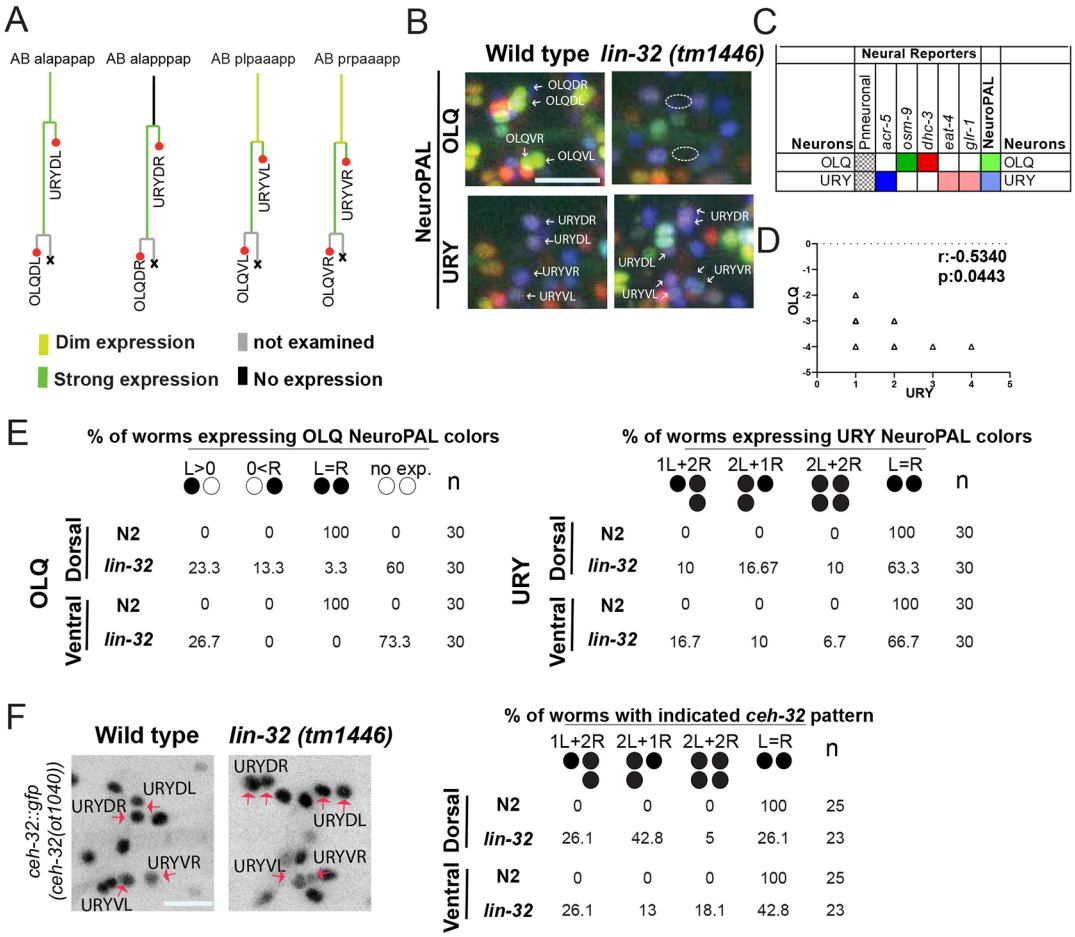

OLQ		L>0	0<R	L=R	no exp.	n
Dorsal	N2	0	0	100	0	30
	lin-32	23.3	13.3	3.3	60	30
Ventral	N2	0	0	100	0	30
	lin-32	26.7	0	0	73.3	30

URY		1L+2R	2L+1R	2L+2R	L=R	n
Dorsal	N2	0	0	0	100	30
	lin-32	10	16.67	10	63.3	30
Ventral	N2	0	0	0	100	30
	lin-32	16.7	10	6.7	66.7	30

		1L+2R	2L+1R	2L+2R	L=R	n
Dorsal	N2	0	0	0	100	25
	lin-32	26.1	42.8	5	26.1	23
Ventral	N2	0	0	0	100	25
	lin-32	26.1	13	18.1	42.8	23

Fig. 9. OLQ-to-URY identity transformation in *lin-32*-null mutants. (A) Lineage diagrams of the expression of *lin-32* in lineages giving birth to URY and OLQ neurons. (B) Terminal identity of OLQ and URY neurons marked by NeuroPAL (*otIs669*). In *lin-32(tm1446)* mutants, there are ectopic signals for the terminal markers of URY (indicated by arrows), whereas the OLQ specific signals are lost. Specifically, we observed potential duplicates of URYDR and URYVR in these mutants. The white-dashed circles outline the position of defective cells. (C) The combination of different reporter colors mixed in the NeuroPAL strain used to mark URY and OLQ neurons. (D) Correlation between the gain in URY terminal markers and loss of OLQ terminal markers. URY and OLQ are lineal cousins and their gain-loss correlation is statistically significant (Pearson correlation, r=−0.534). The negative correlation value reflects the anticorrelated relationship between the observation of both types of neuron (i.e. observing URY is correlated with not observing its lineal cousin OLQ). (E) Percentage of NeuroPAL color codes observed in *lin-32(tm1446)* compared with wild type, using the NeuroPAL reporter (*otIs669*). The OLQ color code in ventral and dorsal OLQ neurons is partially lost in *lin-32* mutants. URY color codes are observed in additional cells in *lin-32* mutants. Circles indicate bilateral homologs of the respective neuron class (L>0, expression only in left neuron; 0<R, expression only in right neuron; L=R, expression in both neurons, i.e. wild type; 2R or 2L, expression in an additional neuron on left or right). (F) Ectopic OLQ expression of the *ceh-32* reporter allele (*ot1040*), normally expressed in URY indicated by red arrows (and identified via NeuroPAL). The percentage of animals that displayed *ceh-32* reporter allele expression is shown on the right. Circles indicate bilateral homologs of the respective neuron class (L>0: expression only in left neuron; 0<R: expression only in right neuron; L=R: expression in both neurons, i.e. wild type). Scale bars: 10 µm.

Similarly, *lin-32* may promote the expression of a terminal selector in the OLQ neuron that not only induces OLQ identity, but may also repress *ceh-32*-induced URY fate; hence, loss of *lin-32* may result in an OLQ-to-URY identity transformation.

Moving beyond *lin-32*, we have also examined here the expression pattern of other Ato superfamily genes (*ngn-1/Neurogenin* and *cnd-1/NeuroD*), as well as proneural AS-C homologs, thereby providing a broad, panoramic view of how these genes may affect neurogenesis in *C. elegans*. We observed patterns that are reminiscent of those reported in flies and vertebrates (Baker and Brown, 2018; Bertrand et al., 2002; Hassan and Bellen, 2000): (1) individual Ato- and AS-C homologs are selectively expressed in distinct neuronal lineages; and (2) with some notable exceptions (Masoudi et al., 2018), they are expressed transiently during early stages of neurogenesis and, therefore, reflect a transient regulatory state that is located between neuronal fate specification and terminal differentiation.

In conclusion, we have provided insights into how terminal differentiation programs in the nervous system, controlled by terminal selector transcription factors, are coupled to earlier developmental events and, specifically, to the lineage history of a cell. Our findings demonstrate that terminal selectors are key integrators of lineage history and provide novel perspectives on how bHLH genes function to pattern the nervous system.

MATERIALS AND METHODS

Strains

Strains were maintained by standard methods (Brenner, 1974). Previously described strains used in this study were as follows:

Mutant alleles: *lin-32(tm1446)* (Doitsidou et al., 2008) and *hlh-14(tm295)* (Poole et al., 2011).

Reporter alleles: *lin-11[ot958(lin-11::gfp::FLAG)]* (Reilly et al., 2020), *ceh-32[ot1040(ceh-32::gfp)]* (kindly provided by Cyril Cros,

Development (2021) 148, dev199224. doi:10.1242/dev.199224

Columbia University, NY, USA), *unc-86[ot879(unc-86::nNeonGreen)]* (Serrano-Saiz et al., 2018) and *unc-42[ot986(unc-42::gfp)]* (Berghoff et al., 2021).

Reporter transgenes: *nIs394 (ngn-1::gfp)* (Nakano et al., 2010), *otIs339 (ceh-43^{fosmid}::gfp)* (Doitsidou et al., 2013), *otIs703[Is(flp-3::mCherry)]; myIs13 (Is[klp-6::gfp])* (kindly provided by Maryam Majeed, Columbia University, NY, USA), NeuroPAL (*otIs669*) (Yemini et al., 2021), *otIs356 [Is(rab-3::NLS::tagRFP)]* (Serrano-Saiz et al., 2013), *lqIs4 [ceh-10p::GFP+lin-15(n765)] X* (kindly provided by Erik Lundquist, University of Kansas, Lawrence, USA) and UL1692: *unc-119(ed3); IeEx1692 {Ex [hlh-34::gfp, unc-119(+)]}* (Cunningham et al., 2012).

Fosmid-based reporters for *hlh-3*, *hlh-14*, *lin-32* and *cnd-1* were generated by insertion of *gfp* at the 3′ end of their respective loci using fosmid recombineering (Sarov et al., 2012). Fosmid names are indicated in the figures. All fosmids were injected into N2 as complex arrays at a concentration of 20 ng/µl with 5 ng/µl of *ttx-3::mCherry* as a co-injection marker and up to 85 ng/µl of OP50 DNA, and then chromosomally integrated. The array names were: *otIs594 (lin-32^{fosmid}::gfp)*, *otIs648 (hlh-3^{fosmid}::gfp)*, *otIs713 (hlh-14^{fosmid}::gfp)* and *otIs813 (cnd-1^{fosmid}::gfp)*.

Microscopy

For fluorescence microscopy, worms were paralyzed by 25 mM sodium azide (NaN_3) and mounted on a 5% agarose pad on glass slides. Images were acquired using an axioscope (Zeiss, AXIO Imager Z.2) or a LSM 800 laser point scanning confocal microscope (Zeiss). Representative images are maximum projections of *z*-stacks. Image reconstruction was performed using Fiji software (ImageJ) (Schindelin et al., 2012).

4D microscopy and SIMI BioCell (Schnabel et al., 1997) was used, as previously described, to analyze embryonic-lineage defects of mutant animals as well as bHLH fosmid reporter expression patterns during embryogenesis. Briefly, gravid adults were dissected on glass slides and a single two-cell-stage embryo was mounted and recorded over 8 h of embryonic development. Nomarski stacks were taken every 30 s and embryos were illuminated with LED fluorescence light (470 nm) at set time points during development. The recording was performed with a Zeiss Imager Z1 compound microscope, using the 4D microscopy software Steuerprg (Caenotec).

Neuron identification using NeuroPAL

We used NeuroPAL, a transgene that expresses 39 neuron type-specific markers and four pan-neuronal drivers (Yemini et al., 2021), to assess the proper execution of cellular differentiation programs. We previously provided proof-of-concept studies for this approach (Yemini et al., 2021) and, herein, we further detail this approach for *lin-32* mutant animals. First, differences in neuronal differentiation were assessed by scoring of transgene color codes; these were reviewed on a per ganglia basis and, thus, the method reduced to only reviewing gangliar groups of ∼20-30 neurons. Given the approximate positional stereotypy of neurons within the worm nervous system, the problem of cell ID can often be even further reduced by focusing on subquadrants of these ganglia. Within each ganglion (or gangliar subquadrant), many non-altered neurons serve as identifiable landmarks. These identifiable landmarks provide a map that orients researchers so that they can pinpoint mutant-based alterations in any of the remaining potentially altered neurons. Upon first review, we attempted to find by eye all those neurons that expressed LIN-32 within their lineage (looking for cell-autonomous changes). Whenever we were unable to find any potential matching cell in the vicinity that could account for the neuron we were looking for, we noted the neuron as altered. This reduced the question for each of these neurons to the following: was the cellular color code missing or had the cell simply changed its coloring? Missing color codes were easy to spot because the NeuroPAL colormap remained the same but was simply missing a cell. Conversely, cells with altered coloring stood out because they had no corresponding equivalent in the known color map. Lastly, cell nuclear morphology (shape and size) provided additional information for verifying identity-related hypotheses. For accurate capturing of the color code, it was also important to analyze image stacks, rather than images taken at a single focal plane. This was because neuronal color codes that were out of the plane of focus can be distorted by individual colors being more affected than others (see Fig. S1 for an example).

Acknowledgements

We thank Chi Chen for assistance with microinjections to generate strains; Cyril Cros, Maryam Majeed, Emily Berghoff, Nuria Flames, Erik Lundquist, Sarah Finkelstein and Hana Littleford for kindly providing strains; and Iva Greenwald, Richard Poole and members of the Hobert lab for comments on the manuscript.

Competing interests

The authors declare no competing or financial interests.

Author contributions

Conceptualization: N.M., O.H.; Methodology: N.M.; Formal analysis: N.M., E.Y., R.S.; Investigation: N.M., E.Y., R.S.; Data curation: N.M.; Writing - original draft: O.H.; Writing - review & editing: N.M., E.Y.; Visualization: N.M.; Supervision: O.H.; Project administration: O.H.; Funding acquisition: O.H.

Funding

O.H. is an Investigator of the Howard Hughes Medical Institute, which funded this work. Deposited in PMC for release after 12 months.

Peer review history

The peer review history is available online at https://journals.biologists.com/dev/article-lookup/doi/10.1242/dev.199224

References

Arlotta, P. and Hobert, O. (2015). Homeotic transformations of neuronal cell identities. *Trends Neurosci.* **38**, 751-762. doi:10.1016/j.tins.2015.10.005

Baker, N. E. and Brown, N. L. (2018). All in the family: proneural bHLH genes and neuronal diversity. *Development* **145**, dev159426. doi:10.1242/dev.159426

Baumeister, R., Liu, Y. and Ruvkun, G. (1996). Lineage-specific regulators couple cell lineage asymmetry to the transcription of the Caenorhabditis elegans POU gene unc-86 during neurogenesis. *Genes Dev.* **10**, 1395-1410. doi:10.1101/gad.10.11.1395

Berghoff, E., Glenwinkel, L., Bhattacharya, A., Sun, H., Mohammadi, N., Antone, A., Feng, Y., Nguyen, K., Cook, S. J., Wood, J. F. et al. (2021). The Prop1-like homeobox gene unc-42 specifies the identity of synaptically connected neurons. *eLife* (in press).

Bertrand, N., Castro, D. S. and Guillemot, F. (2002). Proneural genes and the specification of neural cell types. *Nat. Rev. Neurosci.* **3**, 517-530. doi:10.1038/nrn874

Bertrand, V. and Hobert, O. (2009). Linking asymmetric cell division to the terminal differentiation program of postmitotic neurons in C. elegans. *Dev. Cell* **16**, 563-575. doi:10.1016/j.devcel.2009.02.011

Bhattacharya, A., Aghayeva, U., Berghoff, E. G. and Hobert, O. (2019). Plasticity of the electrical connectome of C. elegans. *Cell* **176**, 1174-1189.e1116. doi:10.1016/j.cell.2018.12.024

Brenner, S. (1974). The genetics of Caenorhabditis elegans. *Genetics* **77**, 71-94. doi:10.1093/genetics/77.1.71

Brunet, J. F. and Ghysen, A. (1999). Deconstructing cell determination: proneural genes and neuronal identity. *BioEssays* **21**, 313-318. doi:10.1002/(SICI)1521-1878(199904)21:4<313::AID-BIES7>3.0.CO;2-C

Brunet, J. F. and Pattyn, A. (2002). Phox2 genes - from patterning to connectivity. *Curr. Opin. Genet. Dev.* **12**, 435-440. doi:10.1016/S0959-437X(02)00322-2

Cao, J., Spielmann, M., Qiu, X., Huang, X., Ibrahim, D. M., Hill, A. J., Zhang, F., Mundlos, S., Christiansen, L., Steemers, F. J. et al. (2019). The single-cell transcriptional landscape of mammalian organogenesis. *Nature* **566**, 496-502. doi:10.1038/s41586-019-0969-x

Chalfie, M. and Au, M. (1989). Genetic control of differentiation of the Caenorhabditis elegans touch receptor neurons. *Science* **243**, 1027-1033. doi:10.1126/science.2646709

Chan, M. M., Smith, Z. D., Grosswendt, S., Kretzmer, H., Norman, T. M., Adamson, B., Jost, M., Quinn, J. J., Yang, D., Jones, M. G. et al. (2019). Molecular recording of mammalian embryogenesis. *Nature* **570**, 77-82. doi:10.1038/s41586-019-1184-5

Christensen, E. L., Beasley, A., Radchuk, J., Mielko, Z. E., Preston, E., Stuckett, S., Murray, J. I. and Hudson, M. L. (2020). ngn-1/neurogenin activates transcription of multiple terminal selector transcription factors in the caenorhabditis elegans nervous system. *G3 (Bethesda)* **10**, 1949-1962. doi:10.1534/g3.120.401126

Coppola, E., d'Autreaux, F., Rijli, F. M. and Brunet, J. F. (2010). Ongoing roles of Phox2 homeodomain transcription factors during neuronal differentiation. *Development* **137**, 4211-4220. doi:10.1242/dev.056747

Cunningham, K. A., Hua, Z., Srinivasan, S., Liu, J., Lee, B. H., Edwards, R. H. and Ashrafi, K. (2012). AMP-activated kinase links serotonergic signaling to glutamate release for regulation of feeding behavior in C. elegans. *Cell Metab.* **16**, 113-121. doi:10.1016/j.cmet.2012.05.014

Doitsidou, M., Flames, N., Lee, A. C., Boyanov, A. and Hobert, O. (2008). Automated screening for mutants affecting dopaminergic-neuron specification in C. elegans. *Nat. Methods* **5**, 869-872. doi:10.1038/nmeth.1250

Doitsidou, M., Flames, N., Topalidou, I., Abe, N., Felton, T., Remesal, L., Popovitchenko, T., Mann, R., Chalfie, M. and Hobert, O. (2013). A combinatorial regulatory signature controls terminal differentiation of the dopaminergic nervous system in C. elegans. *Genes Dev.* **27**, 1391-1405. doi:10.1101/gad.217224.113

Finney, M. and Ruvkun, G. (1990). The unc-86 gene product couples cell lineage and cell identity in C. *elegans. Cell* **63**, 895-905. doi:10.1016/0092-8674(90)90493-X

Flames, N. and Hobert, O. (2009). Gene regulatory logic of dopamine neuron differentiation. *Nature* **458**, 885-889. doi:10.1038/nature07929

Forrester, W. C., Perens, E., Zallen, J. A. and Garriga, G. (1998). Identification of Caenorhabditis elegans genes required for neuronal differentiation and migration. *Genetics* **148**, 151-165. doi:10.1093/genetics/148.1.151

Frank, C. A., Baum, P. D. and Garriga, G. (2003). HLH-14 is a C. elegans achaete-scute protein that promotes neurogenesis through asymmetric cell division. *Development* **130**, 6507-6518. doi:10.1242/dev.00894

Gordon, P. M. and Hobert, O. (2015). A competition mechanism for a homeotic neuron identity transformation in C. elegans. *Dev. Cell* **34**, 206-219. doi:10.1016/j.devcel.2015.04.023

Hallam, S., Singer, E., Waring, D. and Jin, Y. (2000). The C. elegans NeuroD homolog cnd-1 functions in multiple aspects of motor neuron fate specification. *Development* **127**, 4239-4252. doi:10.1242/dev.127.19.4239

Hassan, B. A. and Bellen, H. J. (2000). Doing the MATH: is the mouse a good model for fly development? *Genes Dev.* **14**, 1852-1865.

Hobert, O. (2014). Development of left/right asymmetry in the Caenorhabditis elegans nervous system: From zygote to postmitotic neuron. *Genesis* **52**, 528-543. doi:10.1002/dvg.22747

Hobert, O. (2016). Terminal selectors of neuronal identity. *Curr. Top. Dev. Biol.* **116**, 455-475. doi:10.1016/bs.ctdb.2015.12.007

Hobert, O., Glenwinkel, L. and White, J. (2016). Revisiting neuronal cell type classification in Caenorhabditis elegans. *Curr. Biol.* **26**, R1197-R1203. doi:10.1016/j.cub.2016.10.027

Hori, S., Oda, S., Suehiro, Y., Iino, Y. and Mitani, S. (2018). OFF-responses of interneurons optimize avoidance behaviors depending on stimulus strength via electrical synapses. *PLoS Genet.* **14**, e1007477. doi:10.1371/journal.pgen.1007477

Jarman, A. P. and Groves, A. K. (2013). The role of Atonal transcription factors in the development of mechanosensitive cells. *Semin. Cell Dev. Biol.* **24**, 438-447. doi:10.1016/j.semcdb.2013.03.010

Masoudi, N., Tavazoie, S., Glenwinkel, L., Ryu, L., Kim, K. and Hobert, O. (2018). Unconventional function of an Achaete-Scute homolog as a terminal selector of nociceptive neuron identity. *PLoS Biol.* **16**, e2004979. doi:10.1371/journal.pbio.2004979

McKenna, A., Findlay, G. M., Gagnon, J. A., Horwitz, M. S., Schier, A. F. and Shendure, J. (2016). Whole-organism lineage tracing by combinatorial and cumulative genome editing. *Science* **353**, aaf7907. doi:10.1126/science.aaf7907

Miller, R. M. and Portman, D. S. (2011). The Wnt/beta-catenin asymmetry pathway patterns the atonal ortholog lin-32 to diversify cell fate in a Caenorhabditis elegans sensory lineage. *J. Neurosci.* **31**, 13281-13291. doi:10.1523/JNEUROSCI.6504-10.2011

Mitani, S., Du, H., Hall, D. H., Driscoll, M. and Chalfie, M. (1993). Combinatorial control of touch receptor neuron expression in Caenorhabditis elegans. *Development* **119**, 773-783. doi:10.1242/dev.119.3.773

Murgan, S., Kari, W., Rothbächer, U., Iché-Torres, M., Mélénec, P., Hobert, O. and Bertrand, V. (2015). Atypical transcriptional activation by TCF via a Zic transcription factor in C. elegans neuronal precursors. *Dev Cell* **33**, 737-745. doi:10.1016/j.devcel.2015.04.018

Murray, J. I., Boyle, T. J., Preston, E., Vafeados, D., Mericle, B., Weisdepp, P., Zhao, Z., Bao, Z., Boeck, M. and Waterston, R. H. (2012). Multidimensional regulation of gene expression in the C. elegans embryo. *Genome Res.* **22**, 1282-1294. doi:10.1101/gr.131920.111

Nakano, S., Ellis, R. E. and Horvitz, H. R. (2010). Otx-dependent expression of proneural bHLH genes establishes a neuronal bilateral asymmetry in C. elegans. *Development* **137**, 4017-4027. doi:10.1242/dev.058834

Packer, J. S., Zhu, Q., Huynh, C., Sivaramakrishnan, P., Preston, E., Dueck, H., Stefanik, D., Tan, K., Trapnell, C., Kim, J. et al. (2019). A lineage-resolved molecular atlas of C. elegans embryogenesis at single-cell resolution. *Science* **365**. doi:10.1126/science.aax1971

Pham, K., Masoudi, N., Leyva-Diaz, E. and Hobert, O. (2021). A nervous system-specific subnuclear organelle in Caenorhabditis elegans. *Genetics* **217**, 1-7. doi:10.1093/genetics/iyaa016

Poole, R. J., Bashllari, E., Cochella, L., Flowers, E. B. and Hobert, O. (2011). A genome-wide RNAi Screen for factors involved in neuronal specification in Caenorhabditis elegans. *PLoS Genet.* **7**, e1002109. doi:10.1371/journal.pgen.1002109

Portman, D. S. and Emmons, S. W. (2000). The basic helix-loop-helix transcription factors LIN-32 and HLH-2 function together in multiple steps of a C. elegans neuronal sublineage. *Development* **127**, 5415-5426. doi:10.1242/dev.127.24.5415

Reilly, M. B., Cros, C., Varol, E., Yemini, E. and Hobert, O. (2020). Unique homeobox codes delineate all the neuron classes of C. elegans. *Nature* **584**, 595-601. doi:10.1038/s41586-020-2618-9

Rojo Romanos, T., Pladevall-Morera, D., Langebeck-Jensen, K., Hansen, S., Ng, L. and Pocock, R. (2017). LIN-32/Atonal controls oxygen sensing neuron development in Caenorhabditis elegans. *Sci. Rep.* **7**, 7294. doi:10.1038/s41598-017-07876-4

Sarov, M., Murray, J. I., Schanze, K., Pozniakovski, A., Niu, W., Angermann, K., Hasse, S., Rupprecht, M., Vinis, E., Tinney, M. et al. (2012). A genome-scale resource for in vivo tag-based protein function exploration in C. elegans. *Cell* **150**, 855-866. doi:10.1016/j.cell.2012.08.001

Schindelin, J., Arganda-Carreras, I., Frise, E., Kaynig, V., Longair, M., Pietzsch, T., Preibisch, S., Rueden, C., Saalfeld, S., Schmid, B. et al. (2012). Fiji: an open-source platform for biological-image analysis. *Nat. Methods* **9**, 676-682. doi:10.1038/nmeth.2019

Schnabel, R., Hutter, H., Moerman, D. and Schnabel, H. (1997). Assessing normal embryogenesis in Caenorhabditis elegans using a 4D microscope: variability of development and regional specification. *Dev. Biol.* **184**, 234-265. doi:10.1006/dbio.1997.8509

Serrano-Saiz, E., Poole, R. J., Felton, T., Zhang, F., De La Cruz, E. D. and Hobert, O. (2013). Modular control of glutamatergic neuronal identity in C. elegans by distinct homeodomain proteins. *Cell* **155**, 659-673. doi:10.1016/j.cell.2013.09.052

Serrano-Saiz, E., Leyva-Díaz, E., De La Cruz, E. and Hobert, O. (2018). BRN3-type POU homeobox genes maintain the identity of mature postmitotic neurons in nematodes and mice. *Curr. Biol.* **28**, 2813-2823.e2812. doi:10.1016/j.cub.2018.06.045

Shaham, S. and Bargmann, C. I. (2002). Control of neuronal subtype identity by the C. elegans ARID protein CFI-1. *Genes Dev.* **16**, 972-983. doi:10.1101/gad.976002

Smit, R. B., Schnabel, R. and Gaudet, J. (2008). The HLH-6 transcription factor regulates C. elegans pharyngeal gland development and function. *PLoS Genet.* **4**, e1000222. doi:10.1371/journal.pgen.1000222

Stefanakis, N., Carrera, I. and Hobert, O. (2015). Regulatory logic of pan-neuronal gene expression in C. elegans. *Neuron* **87**, 733-750. doi:10.1016/j.neuron.2015.07.031

Sulston, J. E. and Horvitz, H. R. (1977). Post-embryonic cell lineages of the nematode, Caenorhabditis elegans. *Dev. Biol.* **56**, 110-156. doi:10.1016/0012-1606(77)90158-0

Sulston, J. E., Schierenberg, E., White, J. G. and Thomson, J. N. (1983). The embryonic cell lineage of the nematode Caenorhabditis elegans. *Dev. Biol.* **100**, 64-119. doi:10.1016/0012-1606(83)90201-4

Taylor, S. R., Santpere, G., Weinreb, A., Barrett, A., Reilly, M., Xu, C., Verdol, E., Oikonomou, P., Glenwinkel, L., McWhirter, R. et al. (2021). Molecular topography of an entire nervous system. *Cell* (in press).

Topalidou, I. and Chalfie, M. (2011). Shared gene expression in distinct neurons expressing common selector genes. *Proc. Natl. Acad. Sci. USA* **108**, 19258-19263. doi:10.1073/pnas.1111684108

Vidal, B., Santella, A., Serrano-Saiz, E., Bao, Z., Chuang, C. F. and Hobert, O. (2015). C. elegans SoxB genes are dispensable for embryonic neurogenesis but required for terminal differentiation of specific neuron types. *Development* **142**, 2464-2477. doi:10.1242/dev.125740

Wagner, D. E., Weinreb, C., Collins, Z. M., Briggs, J. A., Megason, S. G. and Klein, A. M. (2018). Single-cell mapping of gene expression landscapes and lineage in the zebrafish embryo. *Science* **360**, 981-987. doi:10.1126/science.aar4362

Way, J. C. and Chalfie, M. (1988). mec-3, a homeobox-containing gene that specifies differentiation of the touch receptor neurons in C. elegans. *Cell* **54**, 5-16. doi:10.1016/0092-8674(88)90174-2

Wenick, A. S. and Hobert, O. (2004). Genomic cis-regulatory architecture and trans-acting regulators of a single interneuron-specific gene battery in C. elegans. *Dev. Cell* **6**, 757-770. doi:10.1016/j.devcel.2004.05.004

White, J. G., Southgate, E., Thomson, J. N. and Brenner, S. (1986). The structure of the nervous system of the nematode *Caenorhabditis elegans. Philos. Trans. R. Soc. Lond. B Biol. Sci.* **314**, 1-340. doi:10.1098/rstb.1986.0056

Yemini, E., Lin, A., Nejatbakhsh, A., Varol, E., Sun, R., Mena, G. E., Samuel, A. D. T., Paninski, L., Venkatachalam, V. and Hobert, O. (2021). NeuroPAL: a multicolor atlas for whole-brain neuronal identification in C. elegans. *Cell* **184**, 272-288.e211. doi:10.1016/j.cell.2020.12.012

Zhang, A., Noma, K. and Yan, D. (2020). Regulation of Gliogenesis by lin-32/Atoh1 in Caenorhabditis elegans. *G3 (Bethesda)* **10**, 3271-3278. doi:10.1534/g3.120.401547

Zhang, F., Bhattacharya, A., Nelson, J. C., Abe, N., Gordon, P., Lloret-Fernandez, C., Maicas, M., Flames, N., Mann, R. S., Colon-Ramos, D. A. et al. (2014). The LIM and POU homeobox genes ttx-3 and unc-86 act as terminal selectors in distinct cholinergic and serotonergic neuron types. *Development* **141**, 422-435. doi:10.1242/dev.099721

Zhao, C. and Emmons, S. W. (1995). A transcription factor controlling development of peripheral sense organs in C. elegans. *Nature* **373**, 74-78. doi:10.1038/373074a0

Zhu, Z., Liu, J., Yi, P., Tian, D., Chai, Y., Li, W. and Ou, G. (2014). A proneural gene controls C. elegans neuroblast asymmetric division and migration. *FEBS Lett.* **588**, 1136-1143. doi:10.1016/j.febslet.2014.02.036

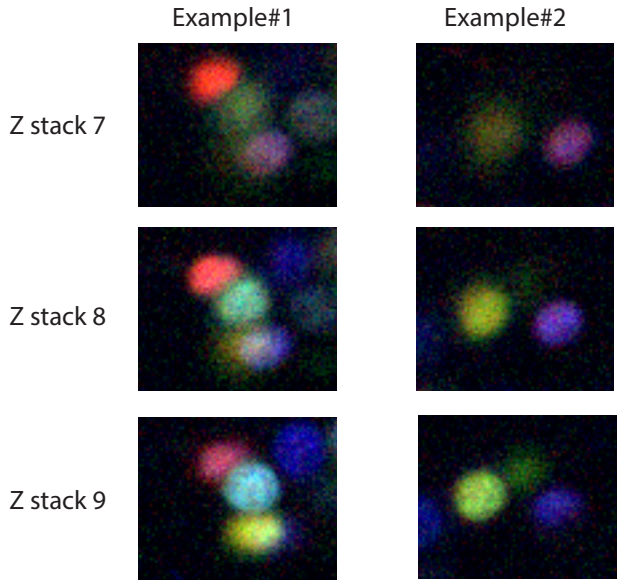

Fig. S1: Example of NeuroPal color change in different plane of focus. This example demonstrates how images presented at single focal planes can lead to misleading color code alterations in NeuroPAL images (see Methods). Hence, cell identifications cannot be done by using single focal planes, but requires the analysis of multi-focal image stacks.

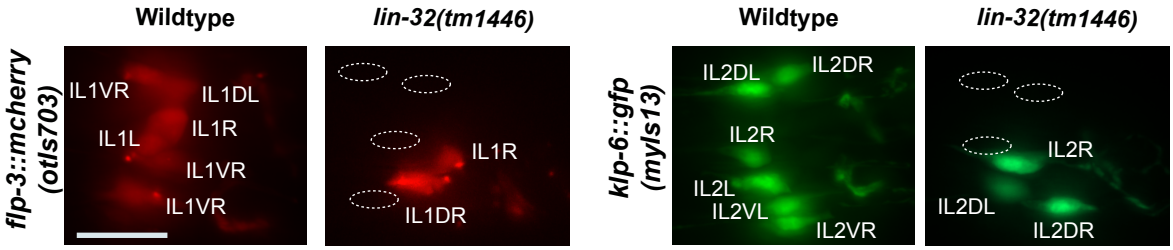

flp-3::mcherry IL1		% of worms L>0 ●○	0<R ○●	L=R ●●	no exp. ○○	n
Dorsal	N2	0	0	100	0	30
	lin-32	0	27.1	0	72.9	48
Lateral	N2	0	0	100	0	30
	lin-32	14.8	3.7	0	81.5	48
Ventral	N2	0	0	100	0	30
	lin-32	7.4	3.7	88.9	0	48

klp-6::gfp IL2		% of worms L>0 ●○	0<R ○●	L=R ●●	no exp. ○○	n
Dorsal	N2	0	0	100	0	30
	lin-32	29.2	45.8	0	25	48
Lateral	N2	0	0	100	0	30
	lin-32	12.5	29.2	0	45.8	48
Ventral	N2	0	0	100	0	30
	lin-32	0	0	100	0	48

Fig. S2: Additional effects of *lin-32/Ato* on marker gene expression. The terminal identity of IL1 and IL2 neurons are affected in *lin-32(tm1446),* shown here using *flp-3::mCherry* and *klp-6::gfp* reporters. Quantification is shown in lower panels. Circles indicate bilateral homologs of the respective neuron class (L>0: Expression only in left neuron; 0<R: expression only in right neuron; L=R: expression in both neurons = wildtype).

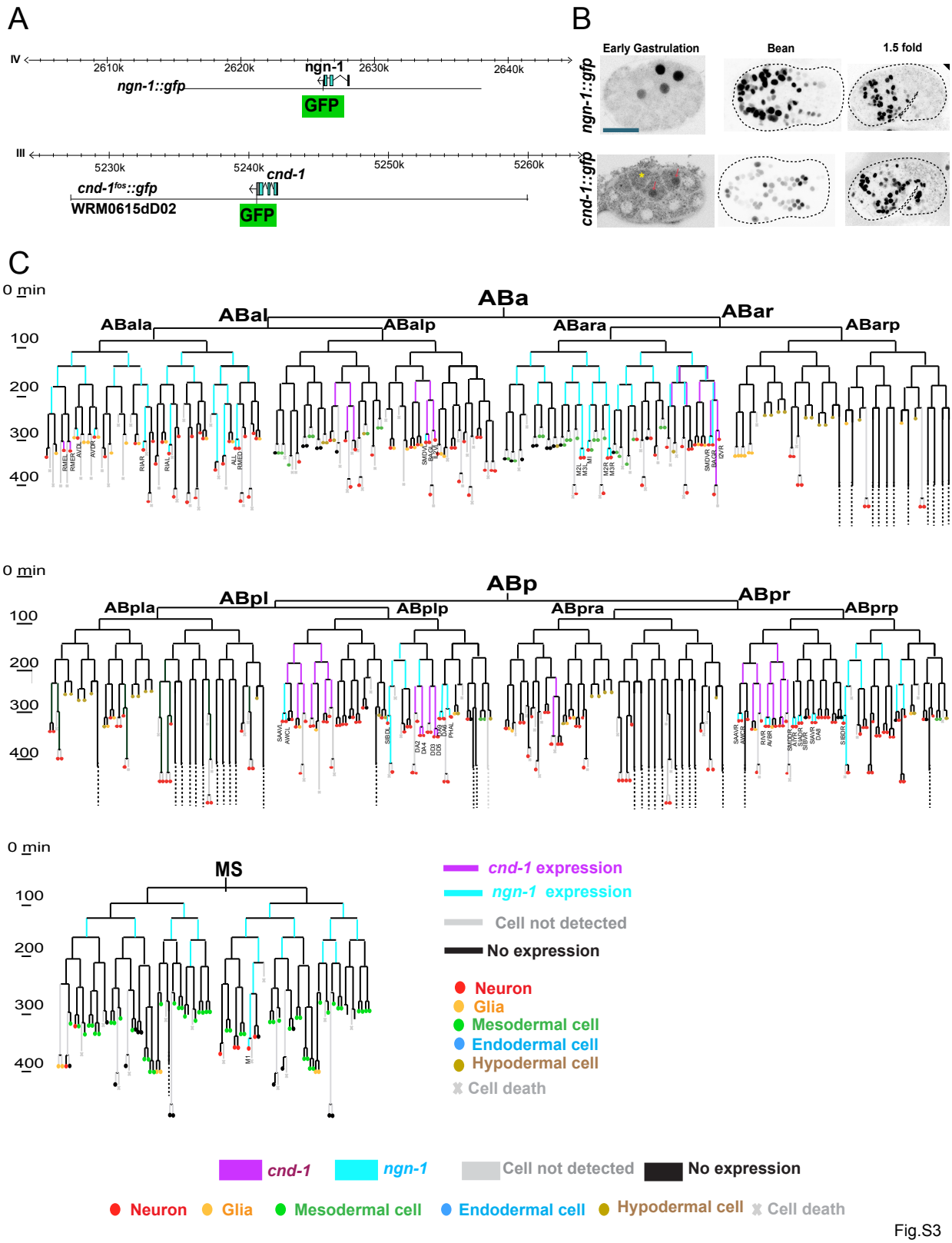

Fig.S3

Fig. S3: Embryonic expression of the *C. elegans* neurogenin and NeuroD homologs, *ngn-1* and *cnd-1*. A: Schematic of gene structure and the fosmid used for expression pattern analysis. **B:** Representative images of *cnd-1* (*otIs813) and ngn-1 (nIs394)* gene expression at embryonic stages, starting from the earliest stage where the expression

starts and continuing to the time when all terminal neurons have been born. Yellow asterisk is marking the cytoplasmic autofluorescence and red arrows are pointing toward real expression inside nuclei. **C:** The full lineage of *cnd-1 and ngn-1* expression in the AB and MS lineages; these lineages produce all but 2 of the 302 neurons in adult *C. elegans* hermaphrodites. Our analysis confirms previously published expression patterns reported for a subset of the cells shown here (Hallam et al., 2000; Nakano et al., 2010).